AGU PUBLICATIONS

JGR

Journal of Geophysical Research: Solid Earth

RESEARCH ARTICLE
10.1002/2014JB011368

Key Point:
- Passive degassing depressurizes magma reservoirs by several MPa

Supporting Information:
- Readme
- Figure S2
- Figure S3
- Figure S4
- Figure S5
- Figure S6
- Figure S7

Correspondence to:
T. Girona,
tarsilo.girona@gmail.com

Citation:
Girona, T., F. Costa, C. Newhall, and B. Taisne (2014), On depressurization of volcanic magma reservoirs by passive degassing, *J. Geophys. Res. Solid Earth*, *119*, doi:10.1002/2014JB011368.

Received 9 JUN 2014
Accepted 22 OCT 2014
Accepted article online 28 OCT 2014

On depressurization of volcanic magma reservoirs by passive degassing

Társilo Girona[1], Fidel Costa[1], Chris Newhall[1], and Benoit Taisne[1]

[1]Earth Observatory of Singapore, Nanyang Technological University, Singapore

Abstract Many active volcanoes around the world alternate episodes of unrest and mildly explosive eruptions with quiescent periods dominated by abundant but passive gas emissions. These are the so-called persistently degassing volcanoes, and well-known examples are Mayon (Philippines) and Etna (Italy). Here, we develop a new lumped-parameter model to investigate by how much the gas released during quiescence can decrease the pressure within persistently degassing volcanoes. Our model is driven by the gas fluxes measured with monitoring systems and takes into account the size of the conduit and reservoir, the viscoelastic response of the crust, the magma density change, the bubble exsolution and expansion at depth, and the hydraulic connectivity between reservoirs and deeper magma sources. A key new finding is that, for a vast majority of scenarios, passive degassing reduces the pressure of shallow magma reservoirs by several MPa in only a few months or years, that is, within the intereruptive timescales of persistently degassing volcanoes. Degassing-induced depressurization could be responsible for the subsidence observed at some volcanoes during quiescence (e.g., at Satsuma-Iwojima and Asama, in Japan; Masaya, in Nicaragua; and Llaima, in Chile), and could play a crucial role in the onset and development of the physical processes which may in turn culminate in new unrest episodes and eruptions. For example, degassing-induced depressurization could promote magma replenishment, induce massive and sudden gas exsolution at depth, and trigger the collapse of the crater floor and reservoir roof.

1. Introduction

Some of the most active volcanoes around the world are the so-called persistently degassing volcanoes (e.g., Mayon, Philippines; Masaya, Nicaragua; and Etna, Italy). Their activity consists of unrest episodes, sometimes culminating in mildly explosive eruptions, which alternate with periods of steady passive gas emissions lasting for a few months or years [e.g., *Shinohara*, 2008; *Siebert et al*., 2010]. The amount of gas released during these passive periods can be constrained by measuring the fluxes of the predominant volcanic gases (H_2O, CO_2, and SO_2) in volcanic plumes and high temperature fumaroles [e.g., *Stoiber et al*., 1983; *Symonds et al*., 1994; *Andres and Kasgnoc*, 1998; *Oppenheimer et al*., 1998; *Galle et al*., 2002; *Aiuppa et al*., 2007; *Sawyer et al*., 2008; *Johansson et al*., 2009; *Boichu et al*., 2010; *Galle et al*., 2010]. These measurements show that persistently degassing volcanoes like Stromboli can release passively up to 6,000–12,000 t/d of gas [*Allard et al*., 1994], Etna emits up to 21,000 t/d [*Aiuppa et al*., 2008], and Masaya and Satsuma-Iwojima volcanoes release about 14,000–16,000 t/d [*Burton et al*., 2000; *Kazahaya et al*., 2002; *Martin et al*., 2010].

Steady gas fluxes of several kilotonnes per day during months or years of quiescence have been explained through two different approaches. In the first approach, gas-magma separation occurs at shallow levels at the top of an open magma conduit. In this case, mean degassing rates are mostly limited by the rate at which volatiles are transported from the magma reservoir to shallow levels, which can occur via steady state magma convection in the conduit [e.g., *Kazahaya et al*., 1994; *Stevenson and Blake*, 1998; *William-Jones et al*., 2003; *Harris et al*., 2005; *Burton et al*., 2007; *Shinohara and Tanaka*, 2012]. In the second approach, gas-magma separation occurs at deep levels within a magma reservoir. In this case, mean degassing rates are mostly limited by the transport of volatiles within the reservoir [e.g., *Simakin and Botcharnikov*, 2001], the ascent velocity of bubbles through the magma [e.g., *Vergniolle and Jaupart*, 1986; *Pioli et al*., 2012], or the permeability of the magma conduit [e.g., *Edmonds et al*., 2001; *Okumura et al*., 2008; *Divoux et al*., 2011; *Polacci et al*., 2012]. Despite all these studies focused on passive degassing, only a few researchers have suggested that the gas lost during quiescence could decrease significantly the pressure within magma plumbing systems [*Simakin and Botcharnikov*, 2001; *Iguchi et al*., 2002].

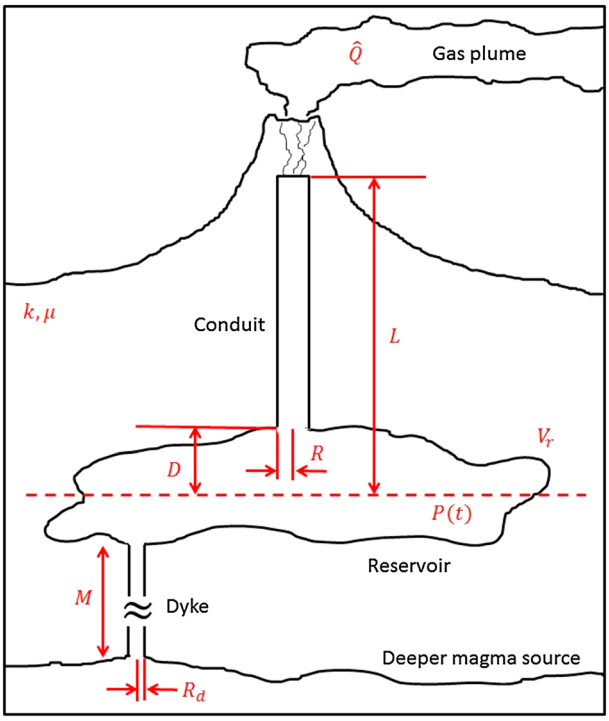

Figure 1. Sketch of a persistently degassing volcano illustrating the main features that we incorporate in the model. A magma reservoir is connected to a well-developed open conduit filled with magma up to somewhere close to the surface, such that the pressure in the reservoir is mainly hydrostatic during quiescence. Hence, weight changes within the conduit induced by degassing will cause pressure changes in the reservoir. The reservoir can be hydraulically connected to a deeper magma source through a cylindrical dyke, and gas finally escapes through a crater that can be covered or not by a permeable dome [e.g., *Shinohara*, 2008]. For description of the parameters, see Notation section.

Here, we develop a lumped-parameter model to calculate the magnitude of the pressure drops induced by passive degassing within persistently degassing volcanoes. Our model applies to volcanoes with open conduits and with shallow and deep gas-magma separation levels, and it captures the long-term (from months to years) overall trend of the pressure change. Determining the pressure changes induced by passive degassing is crucial for a better understanding of the evolution of the magma plumbing systems and for improving the interpretation of the monitoring signals of active volcanoes [*Sparks*, 2003].

2. Model Approach and Physical Constraints

Calculating the pressure changes during passive degassing is not straightforward given the complex processes that occur within magmatic systems. For instance, bubbles nucleate and grow, ascend through the melt, and may accumulate beneath viscous magma layers or geometric barriers [e.g., *Sparks*, 1978; *Patrick et al*., 2011]. Viscous foams may form and collapse in the upper part of the conduit or at the reservoir roof, causing rise and fall of the magma level [*Dibble*, 1972; *Jaupart and Vergniolle*, 1988; *Orr and Rea*, 2012], and gas slugs may travel through the conduit generating long and very long period seismicity [e.g., *Vergniolle and Jaupart*, 1986; *James et al*., 2006]. Even more complexities arise if we consider degassing-induced crystallization [*Lipman et al*., 1985; *Metrich et al*., 2001], magma circulation transporting volatiles from the reservoir to the conduit [e.g., *Shinohara*, 2008], magma intrusions from deep sources to the reservoirs [e.g., *Blake*, 1981], or the response of the crust to pressure changes [e.g., *Dzurisin*, 2007]. Here we address the problem by considering the following conditions:

1. An idealized system in which a magma reservoir is connected to an open cylindrical conduit filled with magma (see Figure 1) [e.g., *Shinohara*, 2008; *Tanaka et al*., 2008, 2009]. The depth of magma reservoirs ranges between 3 and 10 km [e.g., *Dzurisin*, 2007], and the radius of the conduit can vary from a few to up to 100 m (5–10 m, Stromboli; 40–60 m, Mount St. Helens; 100 m, Satsuma-Iwojima) [e.g., *Pallister et al*., 1992; *Stevenson and Blake*, 1998, 2009]. The volume of the magma reservoir of a given volcano is typically assumed to be on the same order or one order of magnitude larger than the volume of magma extruded in its largest eruptions [e.g., *Dzurisin*, 2007; *Siebert et al*., 2010]. Therefore, reservoir volumes of persistently degassing volcanoes likely range between 10^7 and 10^9 m^3, even though a larger reservoir of 10^{10} m^3 has also been proposed for Masaya [*Walker et al*., 1993].
2. The magma pressure within the reservoir is mainly magmastatic [e.g., *Simakin and Botcharnikov*, 2001]. Hence, the pressure change ΔP in the reservoir can be calculated from the mass change of magma within the conduit. For simplicity, we consider that the whole conduit is subjected to the same pressure change as the reservoir and that the mass of gas inside the conduit is always much lower than the mass of bubble-free magma (liquid and solid phase). In the rest of the paper, we refer to the bubble-free magma as melt, which is considered incompressible.

3. The melt inside the magma conduit is described as a mixture of two melts with different dissolved volatile content and therefore with different densities [e.g., *Stevenson and Blake*, 1998; *Kazahaya et al.*, 2002; *Shinohara*, 2008]. The maximum mass fraction of volatiles that can exsolve and escape from the melt n_x depends on the mechanism of degassing. If gas separation occurs in the reservoir, $n_x \approx n_r$, where n_r is the maximum mass fraction of water that can exsolve at the pressure of the reservoir. If gas separation occurs at shallow levels in the conduit, $n_x \approx n_c$, where n_c is the maximum mass fraction of water that can exsolve at the pressure of the upper part of the conduit. It is satisfied that $n_r < n_c \leq \alpha$, where α is the mass fraction of volatiles that were initially dissolved in the melt (from here on, we refer to the melt prior to gas exsolution as parent melt). We also assume that the mean rate of conversion from the parent melt to the fully degassed melt (i.e., melt that exsolves a mass fraction of volatiles given by n_x) equals the mean degassing rate $\hat{Q}$ [e.g., *Kazahaya et al.*, 1994; *Stevenson and Blake*, 1998].
4. Persistently degassing volcanoes release gas at a mean rate $\hat{Q}$ ranging between 1 and at least 10 kt/d [*Allard et al.*, 1994; *Burton et al.*, 2000; *Kazahaya et al.*, 2002; *Aiuppa et al.*, 2008; *Martin et al.*, 2010]. Mean degassing rates during quiescence are considered constant, and thus we calculate the long-term (from months to years) pressure change in the reservoir due to steady gas loss [*Shinohara*, 2008]. Continuous gas emissions can in principle occur as long as the mass of volatiles released is lower than the mass of volatiles initially dissolved in the conduit-reservoir system.
5. The gas solubility depends only on pressure, and gas exsolution within the reservoir occurs at thermodynamic equilibrium according to Henry's law [e.g., *Huppert and Woods*, 2002]. We consider constant temperature T within the system, neglect crystal content in the reservoir, and calculate the mass of gas within the reservoir considering a given mean depth. (Figure 1). Gas expansion occurs in the reservoir and conduit following the ideal gas law. This allows us to account for the compressibility of bubble-bearing magmas.
6. The volume of melt decreases because of the exsolution of water during passive degassing [*Simakin and Botcharnikov*, 2001]. We neglect volume changes of melt that are due to the exsolution of other less abundant volatiles [e.g., *Allard et al.*, 1994; *Kazahaya et al.*, 2002].
7. The magmatic system is embedded in a half space with a Maxwell viscoelastic rheology characterized by a bulk modulus k and an effective viscosity μ [*Jellinek and DePaolo*, 2003]. This has been successfully used at volcanoes like Long Valley [*Newman et al.*, 2001] or Etna [*Del Negro et al.*, 2009]. The typical value of the bulk modulus of pristine rocks is in the range of $k = 10^{10} - 10^{11}$ Pa [e.g., *Blake*, 1981; *Touloukian et al.*, 1981], and the effective viscosities of the upper crust range between $\mu = 10^{17}$ and 10^{20} Pa s [*Jellinek and DePaolo*, 2003].
8. The reservoir can be permanently connected to a deeper magma source through a narrow cylindrical dyke (up to a few meters radius), which can lead to magma replenishment in the reservoir described by a well-developed Poiseuille flow [e.g., *Pinel et al.*, 2010]. Note that this replenishment is not a requirevment to sustain passive degassing as long as the mass of gas released is not larger than the mass of volatiles that were initially within the conduit-reservoir system [e.g., *Shinohara*, 2008; *Simakin and Botcharnikov*, 2001].

In the following, we derive a time-dependent model that accounts for the mass change by degassing, volume change of the volcanic system, gas expansion at depth, magma density changes, and magma replenishment. With this model, we perform a parametric analysis to assess the effect of passive degassing on the pressure evolution of magma plumbing systems within the intereruptive timescales of persistently degassing volcanoes (<10 years). Then, we discuss the implications of our results.

3. Pressure Change Model for Persistently Degassing Volcanoes During Quiescence

The pressure change with time $\Delta P(t)$ within the magma reservoir can be calculated from the hydrostatic equation as (conditions (1) and (2)):

$$\Delta P(t) = P(t) - P(t_0) = \frac{\left[m_{g,c}(t) + m_{m,c}(t)\right] g}{\pi R(t)^2} - P(t_0) \quad (1)$$

where $P(t)$ and $P(t_0)$ are the pressure in the reservoir at time t and at the reference time $t_0 = 0$, respectively, g is gravity, $R(t)$ is the radius of the conduit, and $m_{g,c}(t)$ and $m_{m,c}(t)$ are the mass of gas and melt within the column of length L, respectively, where the magma can move up and down [e.g., *Jaupart and Vergniolle*, 1988; *Harris*

and Ripepe, 2007; *Boichu et al.*, 2010; *Patrick et al.*, 2011; *Orr and Rea*, 2012]. Note that L comprises of the conduit length and a portion of the magma column D which is within the reservoir (up to the mean depth of the reservoir, see Figure 1). As we will show later, there are several terms needed to calculate $\Delta P(t)$ that depend on the rate of pressure change. Therefore, we take here the time-derivative of equation (1) for convenience, which is given by:

$$\frac{\mathrm{d}\Delta P\,(t)}{\mathrm{d}t} = \frac{g\, m_{m,c}(t)}{\pi R(t)^2}\left\{\frac{1}{m_{m,c}(t)}\left[\frac{\mathrm{d}m_{g,c}(t)}{\mathrm{d}t}+\frac{\mathrm{d}m_{m,c}(t)}{\mathrm{d}t}\right]-\frac{2}{R(t)}\frac{\mathrm{d}R(t)}{\mathrm{d}t}\right\} \tag{2}$$

We have assumed here that $m_{m,c}(t) \gg m_{g,c}(t)$ at any time (condition (2)). Note that $m_{g,c}(t)$ must not be neglected prior to taking the derivative of equation (1) because we would omit the term $\mathrm{d}m_{g,c}(t)/\mathrm{d}t$, which in principle cannot be neglected when compared with $\mathrm{d}m_{m,c}(t)/\mathrm{d}t$. By replacing $m_{m,c}(t)$ by $\hat{\rho}_{m,c}(t)V_{m,c}(t)$ and $m_{g,c}(t)$ by $\hat{\rho}_{g,c}(t)V_{g,c}(t)$, where $\hat{\rho}_{m,c}(t)$ and $\hat{\rho}_{g,c}(t)$ are the mean densities of melt and gas inside the column, respectively, and $V_{m,c}(t)$ and $V_{g,c}(t)$ are the volumes of melt and gas inside the column, respectively, we can obtain:

$$\begin{aligned}\frac{\mathrm{d}\Delta P\,(t)}{\mathrm{d}t} = \frac{g\,\hat{\rho}_{m,c}(t)V_{m,c}(t)}{\pi R(t)^2}\Bigg\{&\frac{1}{\hat{\rho}_{m,c}(t)V_{m,c}(t)}\left[\hat{\rho}_{g,c}(t)\frac{\mathrm{d}V_{g,c}(t)}{\mathrm{d}t}+V_{g,c}(t)\frac{\mathrm{d}\hat{\rho}_{g,c}(t)}{\mathrm{d}t}\right.\\&\left.+\hat{\rho}_{m,c}(t)\frac{\mathrm{d}V_{m,c}(t)}{\mathrm{d}t}+V_{m,c}(t)\frac{\mathrm{d}\hat{\rho}_{m,c}(t)}{\mathrm{d}t}\right]-\frac{2}{R(t)}\frac{\mathrm{d}R(t)}{\mathrm{d}t}\Bigg\}\end{aligned} \tag{3}$$

The volume of gas inside the column of length L can be also written as $V_{g,c}(t) = \pi R(t)^2 L - V_{m,c}(t)$. By replacing this in equation (3), and considering that $\hat{\rho}_{m,c}(t)$ is at least one order of magnitude larger than $\hat{\rho}_{g,c}(t)$, we get:

$$\begin{aligned}\frac{\mathrm{d}\Delta P\,(t)}{\mathrm{d}t} = \frac{g\,\hat{\rho}_{m,c}(t)V_{m,c}(t)}{\pi R(t)^2}\Bigg\{&\frac{1}{\hat{\rho}_{m,c}(t)}\frac{\mathrm{d}\,\hat{\rho}_{m,c}(t)}{\mathrm{d}t}+\frac{\left[\pi R(t)^2 L - V_{m,c}(t)\right]}{\hat{\rho}_{m,c}(t)V_{m,c}(t)}\frac{\mathrm{d}\,\hat{\rho}_{g,c}(t)}{\mathrm{d}t}\\&+\frac{1}{V_{m,c}(t)}\frac{\mathrm{d}V_{m,c}(t)}{\mathrm{d}t}-\left[1-\frac{\pi R(t)^2 L\,\hat{\rho}_{g,c}(t)}{\hat{\rho}_{m,c}(t)V_{m,c}(t)}\right]\frac{2}{R(t)}\frac{\mathrm{d}R(t)}{\mathrm{d}t}\Bigg\}\end{aligned} \tag{4}$$

In the following, we determine each of the derivatives of the right-hand side of equation (4).

3.1. Mean Density of Melt in the Column ($\hat{\rho}_{m,c}(t)$)

The mean density of melt in the magma column $\hat{\rho}_{m,c}(t)$ is approximated by (condition (3)):

$$\hat{\rho}_{m,c}(t) = \gamma_c(t)\rho_{c1} + (1-\gamma_c(t))\rho_{c2} \tag{5}$$

where ρ_{c1} is the density of the more degassed melt in the column and ρ_{c2} is the density of the less degassed (or fully undegassed) melt. The term $\gamma_c(t)$ is the volume fraction of the more degassed melt in the magma column, and it is by definition $\gamma_c(t) = V_{m,c1}(t)/V_{m,c}(t)$, where $V_{m,c1}(t)$ is the volume of the more degassed melt. From equation (5), its derivative, and the definition of $\gamma_c(t)$, the term $d\hat{\rho}_{m,c}(t)/dt$ in equation (4) can be replaced by:

$$\frac{\mathrm{d}\hat{\rho}_{m,c}(t)}{\mathrm{d}t} = \Delta\rho_{1,2}\frac{\mathrm{d}\gamma_c(t)}{\mathrm{d}t} = \frac{\gamma_c(t)\Delta\rho_{1,2}}{V_{m,c}(t)}\left[\frac{1}{\gamma_c(t)}\frac{\mathrm{d}V_{m,c1}(t)}{\mathrm{d}t}-\frac{\mathrm{d}V_{m,c}(t)}{\mathrm{d}t}\right] \tag{6}$$

where $\Delta\rho_{1,2} = \rho_{c1} - \rho_{c2}$. The value of $\gamma_c(t)$, and hence the value of $\hat{\rho}_{m,c}(t)$, depends on the mechanism of degassing. For volcanoes in which gas-magma separation occurs in the reservoir and bubbles escape through a permeable degassed magma conduit [e.g., *Pioli et al.*, 2012; *Divoux et al.*, 2011], the volume fraction of the more degassed melt in the column is constant, and therefore, $d\hat{\rho}_{m,c}(t)/dt \approx 0$ and $\hat{\rho}_{m,c}(t)$ is constant. For volcanoes in which gas-magma separation occurs at shallow levels via steady state convection in the conduit, $\gamma_c(t)$ is also roughly constant since the volume of the fully degassed melt sinking from the conduit to the reservoir is replaced continuously by less degassed melt rising from the reservoir to the conduit [e.g., *Shinohara*, 2008]. In this case, equation (6) is also zero and $\hat{\rho}_{m,c}(t)$ is constant as well.

An end-member case with a maximum change of $\hat{\rho}_{m,c}(t)$ during quiescence would be a volcano in which gas separation occurs at shallow levels without steady state convection in the conduit. In such a case, the system would not be gravitationally stable because the denser melt would be on top, but it might be a realistic possibility since the ability for convection also depends on the radius of the conduit and melt viscosity

[e.g., *Stevenson and Blake*, 1998]. For this scenario, $V_{m,c1}(t)$, $\gamma_c(t)$, and $\hat{\rho}_{m,c}(t)$ increase progressively with time as long as the whole conduit is not degassed. Below we show how to obtain the term $dV_{m,c1}(t)/dt$ of equation (6) for this end-member scenario.

By considering conditions (3) and (4), we can state that:

$$\hat{Q} = -n_x \rho_{nd} \left. \frac{dV_{undeg}}{dt} \right|_d \tag{7}$$

where n_x is the mass fraction of volatiles that can exsolve and escape from the melt at the gas-magma separation level, ρ_{nd} is the density of the parent undegassed melt, and the term $dV_{undeg}/dt|_d$ is the rate of volume change of undegassed melt in the conduit-reservoir system due only to degassing. This means that $dV_{undeg}/dt|_d$ does not account for the increase of undegassed melt because of replenishment. From mass conservation, it is also satisfied that:

$$\rho_x \frac{dV_{deg}(t)}{dt} = -\rho_{nd} \left. \frac{dV_{undeg}}{dt} \right|_d - \hat{Q} \tag{8}$$

where $\rho_x = \rho_{c1}$ when gas separation occurs in the conduit and $\rho_x = \rho_r$ when gas separation occurs in the reservoir, such that ρ_r is the density of the degassed melt of the reservoir. In other words, ρ_x is the melt density at the separation level. The term $dV_{deg}(t)/dt$ is the rate of volume change of fully degassed melt (i.e., melt that has exsolved a mass fraction of volatiles n_x) in the conduit-reservoir system. By combining equations (7) and (8), we get:

$$\frac{dV_{deg}(t)}{dt} = \frac{(1 - n_x)\hat{Q}}{n_x \rho_x} \tag{9}$$

Hence, if we impose that all the melt degasses and stagnates in the conduit, the term $dV_{m,c1}(t)/dt$ takes the form:

$$\frac{dV_{m,c1}(t)}{dt} = \frac{(1 - n_c)\hat{Q}}{n_c \rho_{c1}} \tag{10}$$

In such a case, $\gamma_c(t)$ can be calculated from:

$$\gamma_c(t) = \gamma_c(t_0)\frac{V_{m,c}(t_0)}{V_{m,c}(t)} + \frac{(1 - n_c)\hat{Q}\, t}{n_c \rho_{c1} V_{m,c}(t)} \qquad if \quad V_{m,c1}(t) \le V_{m,c}(t) \tag{11}$$

$$\gamma_c(t) = 1 \qquad if \quad V_{m,c1}(t) > V_{m,c}(t) \tag{12}$$

which is obtained from the definition of $\gamma_c(t)$ and after integrating equation (10). Below we write equation (6) in a compact form that accounts for all the possible scenarios we have mentioned:

$$\frac{d\hat{\rho}_{m,c}(t)}{dt} = \frac{\gamma_c(t)\Delta\rho_{1,2}A^*}{V_{m,c}(t)} \left[\frac{(1 - n_c)\hat{Q}}{\gamma_c(t) n_c \rho_{c1}} - \frac{dV_{m,c}(t)}{dt} \right] \tag{13}$$

where A^* is an indicator variable whose value is 0 when $\hat{\rho}_{m,c}(t)$ and $\gamma_c(t)$ are constants and 1 when the degassed melt accumulates in the column.

3.2. Density of Gas in the Column ($\hat{\rho}_{g,c}(t)$)

If we consider that the pressure change within the column is the same as the pressure change in the reservoir (condition 2) and that the mean density of gas within the column $\hat{\rho}_{g,c}(t)$ can be described with the ideal gas law (condition 5), the term $d\hat{\rho}_{g,c}(t)/dt$ of equation (4) is given by:

$$\frac{d\hat{\rho}_{g,c}(t)}{dt} = \frac{M_{H_2O}}{R_g T} \frac{d\Delta P\,(t)}{dt} \tag{14}$$

where M_{H_2O} is the molecular weight of water, T is the temperature of the magma, and R_g is the universal gas constant.

3.3. Volume of Melt in the Column ($V_{m,c}(t)$)

To calculate the rate of volume change of melt in the column $V_{m,c}(t)$, we can consider that the volume of melt in the conduit-reservoir system $V_m(t)$ is given by:

$$V_m(t) = V_{m,r}(t) + V_{m,c}(t) - \pi R(t)^2 D \tag{15}$$

where $V_{m,r}(t)$ is the volume of melt in the reservoir and D the portion of the magma column which is within the reservoir, as explained above. The last term of equation (15) is included to avoid accounting twice for the volume of melt inside the portion of magma column of length D (see Figure 1). The derivative of $V_m(t)$ is:

$$\frac{dV_m(t)}{dt} = \frac{dV_{m,r}(t)}{dt} + \frac{dV_{m,c}(t)}{dt} - 2\pi R(t) D \frac{dR(t)}{dt} = \frac{dV_d(t)}{dt} + \frac{dV_{rep}(t)}{dt} \tag{16}$$

where $dV_d(t)/dt$ is the rate of volume decrease of melt in the conduit-reservoir system due to gas exsolution and $dV_{rep}(t)/dt$ is the rate of volume increase of melt if there is replenishment. After rearranging terms, $dV_{m,c}(t)/dt$ in equation (4) can be replaced by:

$$\frac{dV_{m,c}(t)}{dt} = \frac{dV_d(t)}{dt} - \frac{dV_{m,r}(t)}{dt} + \frac{dV_{rep}(t)}{dt} + 2\pi R(t) D \frac{dR(t)}{dt} \tag{17}$$

In the next subsections, we determine the first three derivatives of the right-hand side of the equation above.

3.3.1. Volume Decrease of Melt due to Degassing ($V_d(t)$)

The rate of volume decrease of melt because of degassing can be found by rewriting equation (16) as:

$$\frac{dV_m(t)}{dt} = \frac{dV_d(t)}{dt} + \frac{dV_{rep}(t)}{dt} = \frac{dV_{deg}(t)}{dt} + \frac{dV_{undeg}(t)}{dt} \tag{18}$$

where $dV_{undeg}(t)/dt$ is the rate of volume change of the parent undegassed melt in the conduit-reservoir system due to degassing and replenishment. Hence, $dV_{undeg}(t)/dt$ can be written as:

$$\frac{dV_{undeg}(t)}{dt} = \left.\frac{dV_{undeg}(t)}{dt}\right|_d + \frac{dV_{rep}(t)}{dt} \tag{19}$$

The first-term of the right-hand side of equation (19) is the same as in equation (7), and with the second term, we consider that the replenished magma is completely undegassed. By replacing equation (19) in equation (18), and using equations (7) and (9), we get:

$$\frac{dV_d(t)}{dt} = \frac{(1-n_x)\hat{Q}}{n_x \rho_x} - \frac{\hat{Q}}{n_x \rho_{nd}} = -\frac{\hat{Q}}{\rho_w} \tag{20}$$

where we have defined $\rho_w = n_x \rho_x \rho_{nd}/[\rho_x - (1-n_x)\rho_{nd}]$. For $n_x = \alpha$, $\rho_x = \rho_{c1}$, and by neglecting degassing-induced crystallization, the term ρ_w can be interpreted as the partial density of water dissolved in anhydrous melt [*Simakin and Botcharnikov*, 2001].

3.3.2. Volume of Melt Within the Reservoir ($V_{m,r}(t)$)

The volume of melt within the reservoir $V_{m,r}(t)$ depends on the volume of gas that is exsolved at time t in the reservoir $V_{g,r}(t)$ and on the size of the reservoir itself $V_r(t)$. It can be written as:

$$V_{m,r}(t) = V_r(t) - V_{g,r}(t) \tag{21}$$

Therefore, the rate of volume change of melt in the reservoir $dV_{m,r}(t)/dt$ can be calculated from:

$$\frac{dV_{m,r}(t)}{dt} = \frac{dV_r(t)}{dt} - \frac{1}{\hat{\rho}_{g,r}(t)} \frac{dm_{g,r}(t)}{dt} + \frac{m_{g,r}(t)}{\hat{\rho}_{g,r}(t)^2} \frac{d\hat{\rho}_{g,r}(t)}{dt} \tag{22}$$

where $\hat{\rho}_{g,r}(t)$ and $m_{g,r}(t)$ are the mean density and mass of gas in the reservoir, respectively. In the following, we approximate the mass of gas in the reservoir by $m_{g,r}(t) = n_r(t)\rho_{nd}V_r(t)$. By assuming thermodynamic

equilibrium, considering only water vapor (condition 6), and neglecting crystal content, $n_r(t)$ is after Henry's law [e.g., *Huppert and Woods*, 2002]:

$$n_r(t) = \alpha - S\,[P(t_0) + \Delta P(t)]^{1/2} \qquad \text{if} \quad \alpha > S[P(t_0) + \Delta P(t)]^{1/2} \tag{23}$$

$$n_r(t) = 0 \qquad \text{if} \quad \alpha \le S[P(t_0) + \Delta P(t)]^{1/2} \tag{24}$$

where $S = 4 * 10^{-6}\ \mathrm{Pa}^{-1/2}$ for water and $P(t_0)$ is the initial pressure as in equation (1). The actual mass fraction of exsolved volatiles $n_r(t)$ in a magma reservoir could differ from the values given by equation (23) if gas-magma separation occurs at depth. For example, $n_r(t)$ could be larger if some bubbles accumulate progressively with time beneath the reservoir roof [*Jaupart and Vergniolle*, 1988] or could be lower if bubbles can escape from the reservoir very rapidly once they form (the so-called open-system degassing). By using equations (23) and (24), we will gain a first-order insight about the coupling between depressurization induced by degassing and gas exsolution in the reservoir. If we use again the ideal gas law (condition 5), the mean density of gas in the reservoir $\hat{\rho}_{g,r}(t)$ is given by:

$$\hat{\rho}_{g,r}(t) = \frac{[P(t_0) + \Delta P\,(t)]M_{H_2O}}{R_g T} \tag{25}$$

On the other hand, the volume change of the reservoir $V_r(t)$ with time can be described from the generalization of the Maxwell viscoelastic model (condition 7) as [*Jellinek and DePaolo*, 2003]:

$$\frac{\mathrm{d}V_r(t)}{\mathrm{d}t} \approx \frac{V_r(t)}{k}\frac{\mathrm{d}\Delta P\,(t)}{\mathrm{d}t} + \frac{V_r(t)\Delta P\,(t)}{\mu} \tag{26}$$

being k the bulk modulus of rocks and μ the effective viscosity of the crust. Therefore, the time derivative of the melt in the reservoir $\mathrm{d}V_{m,r}(t)/\mathrm{d}t$, after combining the derivatives of equation (23)–(25) with equations (26) and (22), is given by:

$$\begin{aligned}\frac{\mathrm{d}V_{m,r}(t)}{\mathrm{d}t} = &\left\{\left[1 - \frac{n_r(t)\rho_{nd}}{\hat{\rho}_{g,r}(t)}\right]\frac{V_r(t)}{k} + \frac{\rho_{nd}V_r(t)S^2B^*}{2\hat{\rho}_{g,r}(t)(\alpha - n_r(t))} + \frac{n_r(t)\rho_{nd}V_r(t)M_{H_2O}}{\hat{\rho}_{g,r}(t)^2R_gT}\right\}\frac{\mathrm{d}\Delta P(t)}{\mathrm{d}t} \\ &+ \left[1 - \frac{n_r(t)\rho_{nd}}{\hat{\rho}_{g,r}(t)}\right]\frac{V_r(t)}{\mu}\Delta P(t)\end{aligned} \tag{27}$$

where B^* is an indicator variable whose value is 0 if $\alpha \le S[P(t_0) + \Delta P(t)]^{1/2}$, and thus when there are no bubbles in the reservoir ($n_r(t) = 0$), and 1 if $\alpha > S[P(t_0) + \Delta P(t)]^{1/2}$, and thus when there are bubbles in the reservoir ($n_r(t) > 0$).

3.3.3. Volume of Replenished Melt ($V_{rep}(t)$)

If there is connectivity between the reservoir and deep magma sources through dykes [e.g., *Blake*, 1981], magma refilling from deep sources to the reservoir during quiescent periods is possible. If we assume a quasi-steady state approach (condition 8), the volumetric rate of replenished magma can be approximated by the volumetric rate of a well-developed Poiseuille flow inside a dyke [e.g., *Pinel et al.*, 2010]. Thus, we get:

$$\frac{\mathrm{d}V_{\mathrm{rep}}(t)}{\mathrm{d}t} = \lambda(t)(P_s(t) - P(t) - P_{sr}) \tag{28}$$

where $P_s(t)$ is the pressure in the magma source, $P(t)$ is the pressure in the shallow reservoir as in equation (1), and P_{sr} is the hydrostatic pressure exerted on the source by the weight of magma inside the dyke. $\lambda(t)$ is the hydraulic strength of the connectivity between the shallow reservoir and the deep source, which depends on the geometry of the dyke and the rheology of the magma. The above equation can be also written as:

$$\frac{\mathrm{d}V_{\mathrm{rep}}(t)}{\mathrm{d}t} = \lambda(t)(\Delta P_s\,(t) - \Delta P\,(t)) \tag{29}$$

where $\Delta P_s\,(t)$ is the overpressure of the source and is defined as $\Delta P_s(t) = P_s(t) - P(t_0) - P_{sr}$. Equation (29) shows that magma refilling during quiescence at persistently degassing volcanoes can be induced by pressurizations of the deep magma source but also by depressurizations of the shallow reservoir. For a

cylindrical dyke connecting the reservoir with the feeder source and a Newtonian magma rheology, the hydraulic strength is given by [e.g., *Pinel et al*., 2010]:

$$\lambda(t) = \frac{\pi R_d^4}{8M\mu_{nd}} \tag{30}$$

where R_d and M are the radius and the length of the dyke, respectively, and μ_{nd} is the viscosity of the replenished magma (undegassed melt). Magma cooling and crystallization can be important within narrow connecting dykes, which can vary the hydraulic strength $\lambda(t)$ by decreasing the dyke radius, increasing the magma viscosity, and inducing the onset of yield strength in the magma [e.g., *Costa and Macedonio*, 2003; *Melnik and Sparks*, 2005; *Bruce and Huppert*, 1989; *Kavanagh and Sparks*, 2011]. In turn, the cooling rate within the dyke varies with the pressure difference between the magma source and the reservoir [e.g., *Bruce and Huppert*, 1989], and thus, the hydraulic strength also depends on $\Delta P(t)$. A detailed analysis of the coupling between thermal variations within the dykes, and variations of the hydraulic strength depending on $\Delta P(t)$, is beyond the scope of this paper. But we will use equations (28)–(30) to gain a first-order insight about the coupling between depressurization induced by degassing and magma replenishment.

3.4. Radius of the Conduit ($R(t)$)

We calculate the radius change of the conduit by applying the Maxwell viscoelastic approach (equation (26)) to a cylinder (condition 7). In such a case, we get:

$$\frac{\mathrm{d}\pi R(t)^2(L-D)}{\mathrm{d}t} \approx \frac{\pi R(t)^2(L-D)}{k}\frac{\mathrm{d}\Delta P(t)}{\mathrm{d}t} + \frac{\pi R(t)^2(L-D)\,\Delta P(t)}{\mu} \tag{31}$$

And obviating the variations of the length $L-D$, we finally obtain:

$$\frac{\mathrm{d}R(t)}{\mathrm{d}t} \approx \frac{R(t)}{2k}\frac{\mathrm{d}\Delta P(t)}{\mathrm{d}t} + \frac{R(t)\,\Delta P(t)}{2\mu} \tag{32}$$

A more accurate formulation can be found in the literature for the elastic term of the deformation [e.g., *Young and Budynas*, 2002], but our simplification gives the same order of magnitude for the radius change. Hence, we use equation (32) for simplicity.

3.5. The Final Compact Equation

A compact equation for the depressurization rate can be obtained by combining the above equations. If we replace equation (13) in equation (4), we get after rearranging terms:

$$\frac{\mathrm{d}\Delta P(t)}{\mathrm{d}t} = \frac{g\,\hat{\rho}_{m,c}(t)V_{m,c}(t)}{\pi R(t)^2}\left\{\frac{(1-n_c)\hat{Q}\Delta\rho_{1,2}A^*}{n_c\,\rho_{c1}\hat{\rho}_{m,c}(t)V_{m,c}(t)} + \frac{\left[\pi R(t)^2 L - V_{m,c}(t)\right]\mathrm{d}\hat{\rho}_{g,c}(t)}{\hat{\rho}_{m,c}(t)V_{m,c}(t)\quad \mathrm{d}t} + \frac{1}{V_{m,c}(t)}\left(1-\frac{\gamma_c(t)\Delta\rho_{1,2}A^*}{\hat{\rho}_{m,c}(t)}\right)\frac{\mathrm{d}V_{m,c}(t)}{\mathrm{d}t} \quad - \left[1-\frac{\pi R(t)^2 L\hat{\rho}_{g,c}(t)}{\hat{\rho}_{m,c}(t)V_{m,c}(t)}\right]\frac{2\ \mathrm{d}R(t)}{R(t)\ \ \mathrm{d}t}\right\} \tag{33}$$

The term $\gamma_c(t)\Delta\rho_{1,2}A^*/\hat{\rho}_{m,c}(t)$ of the above equation is at least one order of magnitude lower than one, given that $\Delta\rho_{1,2}$ is at least one order of magnitude lower than $\hat{\rho}_{m,c}(t)$ and $\gamma_c(t) \leq 1$. By taking this into account and replacing equation (17) in (33), we get:

$$\frac{\mathrm{d}\Delta P(t)}{\mathrm{d}t} = \frac{g\,\hat{\rho}_{m,c}(t)V_{m,c}(t)}{\pi R(t)^2}\left\{\frac{(1-n_c)\hat{Q}\Delta\rho_{1,2}A^*}{n_c\,\rho_{c1}\hat{\rho}_{m,c}(t)V_{m,c}(t)} + \frac{\left[\pi R(t)^2 L - V_{m,c}(t)\right]\mathrm{d}\hat{\rho}_{g,c}(t)}{\hat{\rho^{}}_{m,c}(t)V_{m,c}(t)\quad \mathrm{d}t} + \frac{1}{V_{m,c}(t)}\left[\frac{\mathrm{d}V_d(t)}{\mathrm{d}t} - \frac{\mathrm{d}V_{m,r}(t)}{\mathrm{d}t} + \frac{\mathrm{d}V_{\mathrm{rep}}(t)}{\mathrm{d}t}\right] - \left[1-\frac{\pi R(t)^2 L\hat{\rho}_{g,c}(t)}{\hat{\rho}_{m,c}(t)V_{m,c}(t)} - \frac{\pi R(t)^2 D}{V_{m,c}(t)}\right]\frac{2\ \mathrm{d}R(t)}{R(t)\ \ Et}\right\} \tag{34}$$

Since $\hat{\rho}_{g,c}(t) \ll \hat{\rho}_{m,c}(t)$, $V_{m,c}(t)$, and $\pi R(t)^2 L$ are on the same order of magnitude, and $D \ll L$, the terms $\pi R(t)^2 L\, \hat{\rho}_{g,c}(t)/\hat{\rho}_{m,c}(t) V_{m,c}(t)$ and $\pi R(t)^2 D\, /V_{m,c}(t)$ are also at least one order of magnitude lower than one. Therefore, by neglecting these terms, and replacing equations (14), (20), (27), (29), and (32) in equation (34), we obtain after rearranging terms:

$$\frac{\mathrm{d}\Delta P\,(t)}{\mathrm{d}t} = \frac{C_1(t) + C_2(t)\Delta P\,(t)}{C_3(t)} \tag{35}$$

being

$$C_1(t) = \left[\frac{(1-n_c)\Delta\rho_{1,2}A^*}{n_c\,\rho_{c1}\hat{\rho}_{m,c}(t)} - \frac{1}{\rho_w}\right]\hat{Q} + \lambda(t)\Delta P_s\,(t) \tag{36}$$

$$C_2(t) = -\left\{\left[1 - \frac{n_r(t)\rho_{nd}}{\hat{\rho_{g,r}}(t)}\right]\frac{V_r(t)}{\mu} + \lambda(t) + \frac{V_{m,c}(t)}{\mu}\right\} \tag{37}$$

$$C_3(t) = \frac{\pi R(t)^2}{g\,\hat{\rho}_{m,c}(t)} + \frac{V_{m,c}(t)}{k} + \left[1 - \frac{n_r(t)\rho_{nd}}{\hat{\rho}_{g,r}(t)}\right]\frac{V_r(t)}{k} + \frac{\rho_{nd}V_r(t)S^2B^*}{2\hat{\rho}_{g,r}(t)(\alpha - n_r(t))} + \left[\frac{n_r(t)\rho_{nd}V_r(t)}{\hat{\rho}_{g,r}(t)^2} - \frac{\pi R(t)^2 L - V_{m,c}(t)}{\hat{\rho}_{m,c}(t)}\right]\frac{M_{H_2O}}{R_gT} \tag{38}$$

The term $\left[\pi R(t)^2 L - V_{m,c}(t)\right]M_{H_2O}/\left[\hat{\rho}_{m,c}(t)R_gT\right]$ of equation (38) is also one order of magnitude lower than the term $\pi R(t)^2/\left[g\,\hat{\rho}_{m,c}(t)\right]$ for typical magma temperatures. Hence, the parameter $C_3(t)$ can be simplified to:

$$C_3(t) = \frac{\pi R(t)^2}{g\,\hat{\rho}_{m,c}(t)} + \frac{V_{m,c}(t)}{k} + \left[1 - \frac{n_r(t)\rho_{nd}}{\hat{\rho}_{g,r}(t)}\right]\frac{V_r(t)}{k} + \frac{\rho_{nd}V_r(t)S^2B^*}{2\hat{\rho}_{g,r}(t)(\alpha - n_r(t))} + \frac{n_r(t)\rho_{nd}V_r(t)M_{H_2O}}{\hat{\rho}_{g,r}(t)^2\quad R_gT} \tag{39}$$

The pressure change with time $\Delta P(t)$ can be calculated by integrating equation (35) from the values of melt density, the size of the conduit and magma reservoir, the mean flux of water vapor, the viscoelastic properties of the host-rock, the hydraulic strength of the connectivity between the reservoir and deeper magma sources, and the gas content in the reservoir (equations (36)–(39)).

3.6. Analytical Solutions

A numerical scheme is required to solve equation (35) in a general case, even though a simple analytical solution can be obtained if we approximate $C_1(t) \approx C_1(t_0)$, $C_2(t) \approx C_2(t_0)$, and $C_3(t) \approx C_3(t_0)$. This can be done by assuming that $\lambda(t)$ and $\Delta P_s\,(t)$ are constant, and if the variations of the terms $n_r(t)$, $\hat{\rho}_{g,r}(t)$, $V_r(t)$, $R(t)$, $\hat{\rho}_{m,c}(t)$, and $V_{m,c}(t)$ are very small compared to their initial values. The terms $n_r(t)$ and $\hat{\rho}_{g,r}(t)$ can be approximated to $n_r(t_0)$ and $\hat{\rho}_{g,r}(t_0)$ if the magnitude of the pressure change $|\Delta P(t)|$ is at least one order of magnitude lower than the initial pressure of the reservoir $P(t_0)$ [see equations (23) and (25)]. This is satisfied for pressure changes of $|\Delta P(t)| \leq 10$ MPa when the mean reservoir depth is $L \geq 3-4$ km. The terms $V_r(t)$ and $R(t)$ can be replaced by $V_r(t_0)$ and $R(t_0)$, respectively, when $k \gg |\Delta P(t)|$ and $\mu \gg |\Delta P(t)|\ (t - t_0)$. This approximation is realistic for the typical values of bulk modulus $k \sim 10^{10}$ Pa, effective viscosities of $\mu \geq 10^{17}$ Pa s, pressure changes of $|\Delta P(t)| \leq 10$ MPa, and periods of passive degassing of $t - t_0 \leq 10$ years (see equations (26) and (32)). The term $\hat{\rho}_{m,c}(t)$ varies at most by an amount given by $\Delta\rho_{1,2}$ (see equation (5)), which in turn is at least one order of magnitude lower than $\hat{\rho}_{m,c}(t)$. The term $V_{m,c}(t)$ can be also replaced by $V_{m,c}(t_0)$ for the conditions cited above, what can be seen from equations (1), and considering that $m_{m,c}(t) \gg m_{g,c}(t)$ at any time (condition (2)). In such a case, we can write $V_{m,c}(t) \approx \pi R(t)^2[P(t_0) + \Delta P(t)]/g\hat{\rho}_{m,c}(t)$, and hence, $V_{m,c}(t)$ can be replaced by $V_{m,c}(t_0)$ when $R(t)$ and $\hat{\rho}_{m,c}(t)$ can be replaced by $R(t_0)$ and $\hat{\rho}_{m,c}(t_0)$, respectively, and when the pressure change $|\Delta P(t)|$ is at least one order of magnitude lower than the initial pressure of the

reservoir $P(t_0)$. Under these conditions, we obtain after integrating equation (35) that the pressure change $\Delta P(t)$ is given by:

$$\Delta P(t) = -\Delta P_\infty \left(1 - e^{-\Gamma t}\right) \tag{40}$$

where ΔP_∞ and Γ are two positive parameters given by $\Delta P_\infty = C_1(t_0)/C_2(t_0)$ and $\Gamma = -C_2(t_0)/C_3(t_0)$, respectively. We have taken into account that $t_0 = 0$. The term ΔP_∞, which depends on the gas flux $\hat{Q}$, is a maximum value to which the pressure change tends asymptotically with time. In other words, ΔP_∞ is an upper bound and larger pressure changes (in absolute value) cannot be reached within intereruptive periods. Combining equation (40) with equations (26) and (32), and integrating, we get an analytical equation for the volume change of the reservoir $\Delta V_r(t)$ and for the radius change of the conduit $\Delta R(t)$:

$$\Delta V_r(t) = -V_r(t_0)\Delta P_\infty \left[\frac{t}{\mu} + \left(\frac{1}{k} - \frac{1}{\Gamma\mu}\right)\left(1 - e^{-\Gamma t}\right)\right] \tag{41}$$

$$\Delta R(t) = -\frac{R(t_0)\Delta P_\infty}{2} \left[\frac{t}{\mu} + \left(\frac{1}{k} - \frac{1}{\Gamma\mu}\right)\left(1 - e^{-\Gamma t}\right)\right] \tag{42}$$

where we have neglected second order terms, i.e., we have replaced $V_r(t)$ by $V_r(t_0)$ and $R(t)$ by $R(t_0)$ in the right-hand side of equations (26) and (32). We can also obtain an analytical expression which links the volume of replenished magma with the gas flux. By combining equations (29) and (40), we obtain:

$$V_{\text{rep}}(t) = \lambda(t_0)\ t\ [\Delta P_s(t_0) + \Delta P_\infty] + \frac{\lambda \Delta P_\infty}{\Gamma}\ \left(1 - e^{-\Gamma t}\right) \tag{43}$$

A simpler analytical expression for the pressure change can be obtained if the effective viscosity of the crust is very high ($\mu \to \infty$) and the hydraulic strength is very small ($\lambda \to 0$). In such a case, we retrieve from equation (40) an expression which applies to a volcano with only elastic response of the host-rock and as long as there is no magma intrusion:

$$\Delta P(t) = -[\Delta P_\infty \Gamma]^*\ t \tag{44}$$

being $[\Delta P_\infty \Gamma]^* = \Delta P_\infty \Gamma$ for $\mu \to \infty$ and $\lambda \to 0$. The term $[\Delta P_\infty \Gamma]^*$ can be used to get a first-order insight on the depressurization rates during passive degassing. For no connectivity between the reservoir and the deeper sources ($\lambda = 0$), no bubbles in the reservoir ($n_r(t) = 0$ and $B^* = 0$), volcanoes with reservoir volumes much larger than conduit volumes ($V_r(t) \gg V_{m,c}(t)$), and constant melt density in the column ($A^* = 0$ and $\hat{\rho}_{m,c}(t) = \hat{\rho}_{m,c}(t_0)$), depressurization by degassing is simply given by:

$$\Delta P(t) = -\frac{g\,\hat{\rho}_{m,c}(t_0)\ k\ \hat{Q}\ t}{\pi R(t_0)^2 \rho_w k + g\rho_w \hat{\rho}_{m,c}(t_0) V_r(t_0)} \tag{45}$$

4. Parametric Analysis

In this section, we explore the influence of the different parameters of our model for four scenarios that are thought to be applicable to persistently degassing volcanoes during quiescence.

1. We first describe the pressure change induced by passive degassing in a bubble-free reservoir that is not connected to deeper magma sources, and for a constant melt density in the column ($n_r(t) = 0$, $\lambda(t) = 0$, $\hat{\rho}_{m,c}(t) = \hat{\rho}_{m,c}(t_0)$). This would correspond to a scenario in which gas-magma separation occurs at low pressures via steady state convection in the conduit [e.g., *Shinohara*, 2008], as has been proposed at volcanoes like Izu-Oshima [*Kazahaya et al*., 1994], Mount St. Helens [*Stevenson and Blake*, 1998], Stromboli [*Stevenson and Blake*, 1998; *Burton et al*., 2007], Satsuma-Iwojima [*Kazahaya et al*., 2002], and Popocatépetl [*Witter et al*., 2005].
2. Then, we analyze the case in which bubbles exsolve in a reservoir that is not connected to deeper magma sources, by keeping also constant the mean density of melt in the column ($n_r(t) \neq 0$, $\lambda(t) = 0$, $\hat{\rho}_{m,c}(t) = \hat{\rho}_{m,c}(t_0)$). This could correspond to a scenario in which gas-magma separation occurs at depth and bubbles can ascend and escape steadily through a vesicular magma conduit, as has been proposed at volcanoes like Stromboli [*Jaupart and Vergniolle*, 1988] and Soufrière Hills [*Edmonds et al*., 2001].

3. We explore the coupling between depressurization by degassing and magma replenishment when there are no bubbles in the reservoir and for constant melt density in the column ($n_r(t) = 0$, $\lambda(t) \neq 0$, $\hat{\rho}_{m,c}(t) = \hat{\rho}_{m,c}(t_0)$). This scenario will give us some insights on how passive degassing may affect magma replenishment, which is thought to occur more or less frequently at persistently degassing volcanoes [e.g., *Shinohara*, 2008].
4. Finally, we explore the end-member scenario in which gas-magma separation occurs in the conduit but the degassed magma is not replaced by undegassed magma via convection. In this case, we assume a bubble-free reservoir that is not connected to deeper magma sources ($n_r(t) = 0$, $\lambda(t) = 0$, $\hat{\rho}_{m,c}(t) \neq \hat{\rho}_{m,c}(t_0)$). This scenario will give us some insights on the maximum effects of the variations of the melt density in the conduit.

For all our calculations we use an andesitic magma composition at T =1000 °C and an oxygen fugacity at the Ni-NiO buffer. Melt densities and viscosities shown in the next figures are calculated at 2.5 kbar and for a given weight ratio of dissolved water by using MELTS thermodynamic algorithm [*Ghiorso and Sack*, 1995]. Using other reference pressures does not change the final results. The values of the parameters vary between those shown in the notation section.

4.1. Scenario 1: Gas-Free Reservoir, No Replenishment, and Constant Mean Density of Melt in the Column ($n_r(t) = 0$, $\lambda(t) = 0$, $\hat{\rho}_{m,c}(t) = \hat{\rho}_{m,c}(t_0)$)

This scenario corresponds to a volcano in which gas exsolution and degassing occurs at low pressures via magma convection in the conduit [*Shinohara*, 2008]. First, we explore independently the influence of the gas flux, reservoir volume, effective viscosity of the crust, and conduit radius for small volcanic systems ($V_r(t_0) = 10^8 - 10^9$ m^3) and for large volcanic systems ($V_r(t_0) = 10^9 - 10^{10}$ m^3). Then, we calculate the expected volume change of the reservoir $\Delta V_r(t)$ and radius change of the conduit $\Delta R(t)$ for a viscoelastic, elastic, and rigid crust (i.e., with no response of the crust to pressure changes). Finally, we calculate the depressurization induced by degassing by accounting for the parameterization proposed by *Stevenson and Blake* [1998] for a convective magma column, which links the mean gas flux with the viscosity of the magma and the conduit radius.

4.1.1. Influence of the Gas Flux, Reservoir Volume, Effective Viscosity of the Crust, and Conduit Radius

For small volcanic systems ($V_r(t_0) = 10^8 - 10^9$ m^3), we find that underpressures of 5–10 MPa can be reached within a few months or years of quiescent degassing for most values of the parameters (Figures 2a–2d). The depressurization rate is roughly constant and proportional to the mean gas flux when the deformation is dominated by elastic effects (see Figure 2a and equation (43)). Variations of the reservoir size within the range $10^8 - 10^9$ m^3 do not have a major influence, and underpressures of 10 MPa are always reached after around one year of passive degassing (Figure 2b). Whereas a pressure decrease of ~10 MPa is reached after around one year for $\mu \geq 10^{18}$ Pa s, it is about 10 MPa after 2 years for $\mu = 10^{17}$ Pa s. The conduit radius has a strong influence on the pressure change, and very small conduit radius leads to significant underpressures very quickly (Figure 2d). For example, a volcano with 10 m conduit radius depressurizes 10 MPa in only a few months, while a volcano with 80 m conduit radius requires almost 4 years to reach the same underpressure. The fact that the depressurization is larger for smaller conduit sections is consistent with the definition of pressure itself (weight over section).

For large volcanic systems ($V_r(t_0) = 10^9 - 10^{10}$ m^3), viscous effects of the crust become more important, such that the depressurization is not linear with time and is not proportional to the mean gas flux (compare Figure 2a and Figure 2e). The pressure evolution is very sensitive to the reservoir volume (contrary to the above scenario; compare Figure 2b and Figure 2f), and small differences in the range $10^9 - 10^{10}$ m^3 cause very significant changes in the depressurization rates. For example, magma reservoirs of $V_r(t_0) = 10^9$ m^3 can decrease the pressure by about 10 MPa after around 1.5 years, whereas a reservoir of $V_r(t_0) = 10^{10}$ m^3 needs around 10 years to depressurize 7 MPa. The pressure evolution is also very sensitive to the effective viscosity of the crust (Figure 2g), but even for very low effective viscosities ($\mu \sim 10^{17}$ Pa s), underpressures of about 2 MPa are reached in the typical intereruptive timescales. Very small conduit radius leads to lower depressurization rates than for smaller reservoirs, even though a pressure decrease of ~7 MPa can be reached after around two years for a conduit radius of 10 m (compare Figure 2d and Figure 2h).

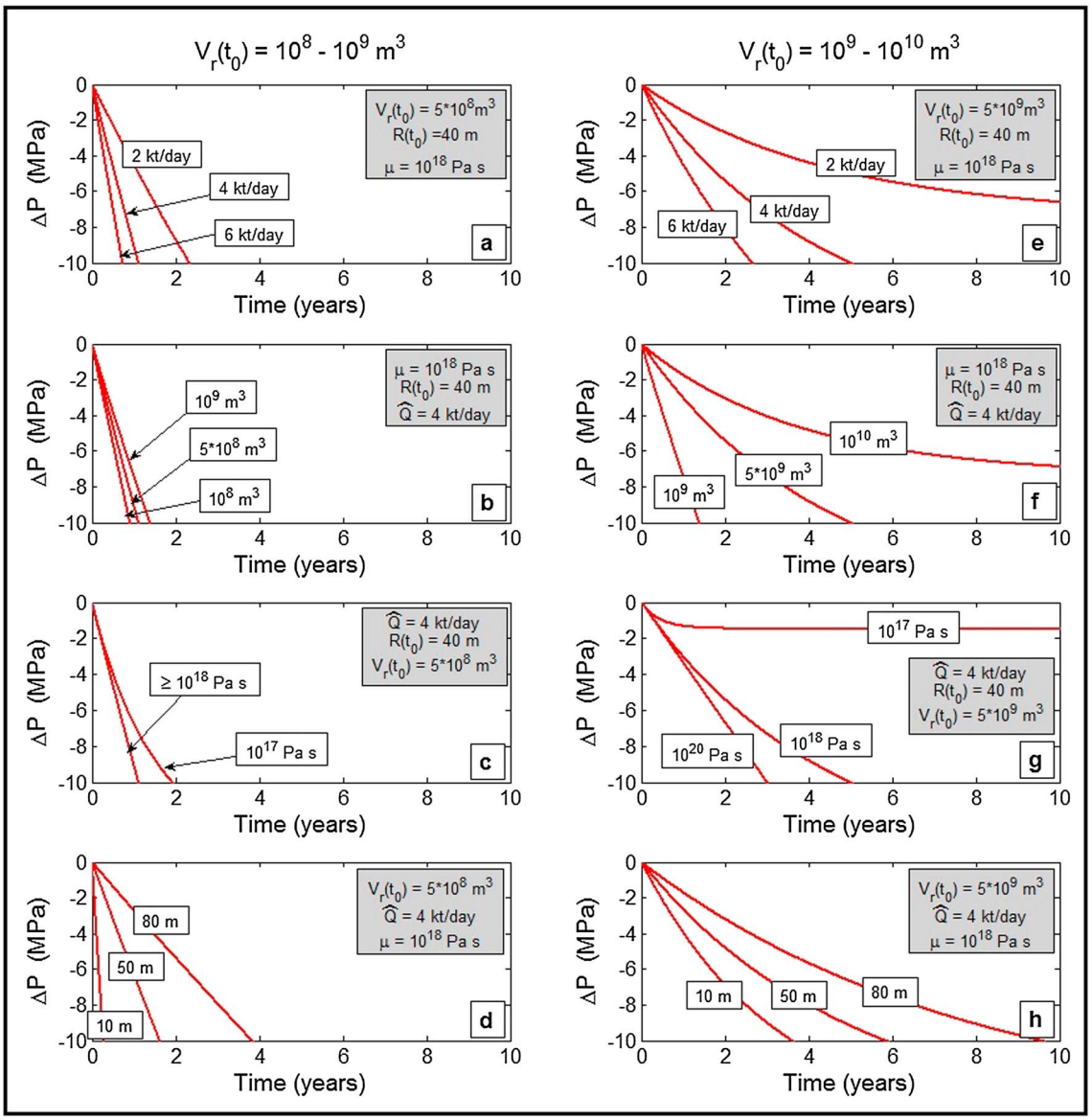

Figure 2. Models of pressure evolution at persistently degassing volcanoes for small ($V_r(t_0) = 10^8 - 10^9$ m^3) and large ($V_r(t_0) = 10^9 - 10^{10}$ m^3) systems. Depressurization for different gas fluxes, (a and e) different reservoir sizes (b and f), different wall-rock viscosities (c and g), and different conduit radius (d and h). We have considered the following: $k = 10^{10}$ Pa,$\alpha = 3$ wt %; $n_x = n_c = 3$ wt % (gas-magma separation at the upper conduit); $\rho_{c1} = 2670$ kg/m^3; $\rho_{c2} = \rho_{nd} = 2430$ kg/m^3; $\gamma_c(t_0) = 0.5$; and $L = 10$ km. With these parameters, $n_r(t) = 0$. It is met that the mass of volatiles released in 10 years or up to $\Delta P = -10$ MPa is lower than the mass of volatiles initially dissolved in an undegassed conduit-reservoir system (i.e., $V_r(t_0)\rho_{nd}\alpha > \hat{Q}t$).

4.1.2. Influence of the Rheology of the Crust: Deformation Induced by Passive Degassing

We explore the change of the pressure, reservoir volume, and conduit radius for a rigid, elastic, and viscoelastic crust. Rigid crust accounts for the end-member case in which pressure changes in magma reservoirs do not deform the volcanic edifice. This could occur for example at highly inhomogenous volcanic environments where deformation is mostly dominated by tectonic stresses.[*Battaglia and Segall*, 2004]. We find that depressurization is linear with time for rigid and elastic wall-rocks (Figure 3a), but rigid environments depressurize much faster than elastic ones (~8 MPa/yr versus ~1 MPa/yr for the parameters we have used in Figure 3). In contrast, the depressurization rate in the viscoelastic regime decreases gradually with time, even though underpressures of several MPa can be still reached after a few years (~3 MPa after 4 years, Figure 3a). The deformation of the reservoir and conduit is larger for the viscoelastic than for the elastic regime, but in both cases, the volume change of the reservoir and the radius change of the conduit induced by passive degassing are on the order of ~ $10^6 - 10^7$ m^3 and ~10 mm, respectively, after a few years. These values represent a

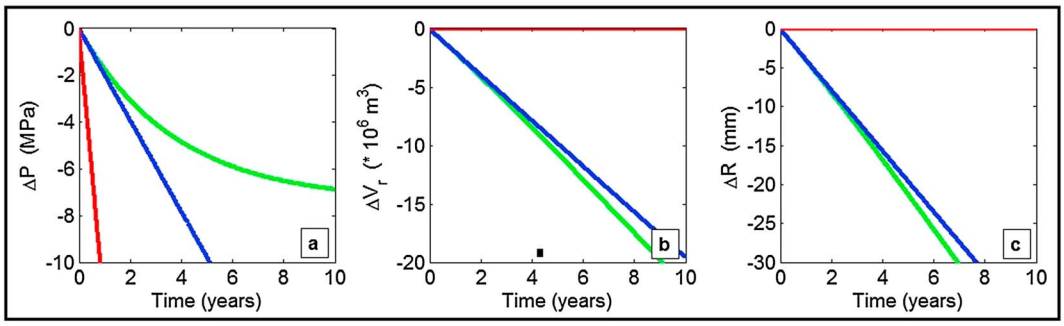

Figure 3. Coupling between degassing-induced depressurization and conduit-reservoir deformation. (a) Pressure change with time with rigid (red), elastic (blue), and viscoelastic (green) host-rock. (b) Volume change of the reservoir with rigid (red), elastic (blue), and viscoelastic (green) host-rock. (c) Radius change of the conduit with rigid (red), elastic (blue), and viscoelastic (green) host-rock. Rigid host-rock: $\mu \to \infty$, $k \to \infty$; elastic host-rock: $\mu \to \infty$, $k = 10^{10}$ Pa; and viscoelastic host-rock $\mu = 10^{18}$ Pa s, $k = 10^{10}$ Pa. For the rest of the parameters, we have used the following: $\hat{Q} = 4$ kt/d, $R(t_0) = 40$ m, $V_r(t_0) = 10^{10}$ m^3; $\alpha = 3$ wt %; $n_x = n_c = 3$ wt % (gas-magma separation at the upper conduit); $\rho_{c1} = 2670$ kg/m^3; $\rho_{c2} = \rho_{nd} = 2430$ kg/m^3; $\gamma_c(t_0) = 0.5$; and $L = 10$ km. With these parameters, $n_r(t) = 0$.

deformation of up to 0.1% for the parameters used in Figures 3b and 3c. An important feature we can extract from Figure 3 is that the lower the ability of a volcanic environment to deform, the larger the depressurization rates induced by degassing. This is because the volume decrease of the reservoir displaces melt into the conduit, which compensates part of the mass decrease of the magma column during degassing.

4.1.3. Link Between Mean Gas Flux, Magma Viscosity, and Conduit Radius

Different types of convection models in a volcanic magma conduit have been used to explain the mean degassing rates of different volcanoes [e.g., *Stevenson and Blake*, 1998; *Burton et al.*, 2007]. In Figure 4, we show the depressurization induced by degassing by assuming that the mean gas flux $\hat{Q}$ is related to the magma viscosity and the conduit radius through the simple parameterization proposed by *Stevenson and Blake* [1998]. This parameterization has been used extensively [e.g., *Kazahaya et al.*, 2002; *Shinohara*, 2008], and it states that the mean gas flux is given by $\hat{Q} \approx \pi (R^*)^2 \xi \left(g \Delta \rho_{1,2} R(t_0)^4 / \mu_1\right)$, where $R^* \approx 0.6$ is an experimental constant, and ξ is the Poiseuille number, which equals to 0.064 when $\mu_1/\mu_{nd} > 12$, being μ_1 the viscosity of the fully degassed melt in the conduit and μ_{nd} the viscosity of the undegassed melt (as in equation (30)). Note that this parameterization linking $\hat{Q}$ with $R(t_0)$ was obtained for a scenario in which the undegassed melt ascends through the conduit to occupy the space left by the denser degassed melt that sinks into the reservoir. In our model, undegassed melt can also rise through the conduit if the reservoir decreases its size, but we still use the same parameterization as a first-order approximation. We obtain that for a realistic mean gas flux between 1.5 and 7.5 kt/d, corresponding to relatively small radius between 10 and 15 m, depressurizations between 2 and 10 MPa are reached after less than five years,

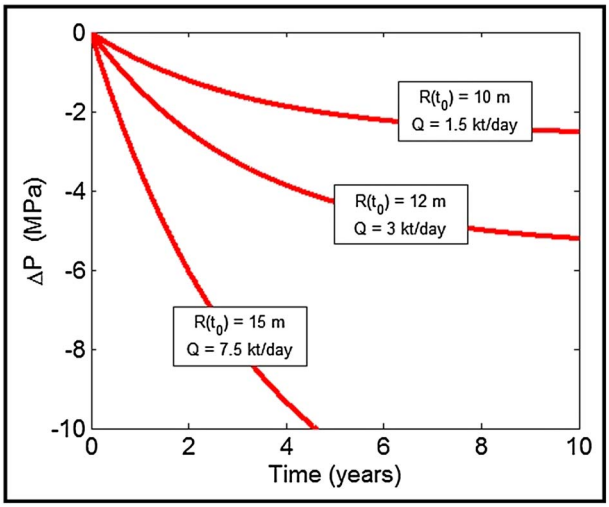

Figure 4. Depressurization by degassing when our model is coupled with the parameterization for magma convection in a conduit proposed by *Stevenson and Blake* [1998]. Red lines correspond to different gas fluxes limited by the conduit radiusdensity difference between the degassed and undegassed melt and the viscosity of the degassed melt (see text for details). For the rest of the parameters, we have used the following: $V_r(t_0) = 5 \times 10^9$ m^3, $\alpha = 3$ wt %, $n_x = n_c = 1.5$ wt % (gas-magma separation at the upper conduit), $\mu_1 = 10^{4.9}$ Pa s, $\mu_{nd} = 10^{3.3}$ Pa s, $\rho_{c1} = 2530$ kg/m^3, $\rho_{c2} = \rho_{nd} = 2430$ kg/m^3, $\gamma_c(t_0) = 0.5$, $\mu = 10^{18}$ Pa s, $k = 10^{10}$ Pa, and $L = 10$ km. With these parameters, $n_r(t) = 0$.

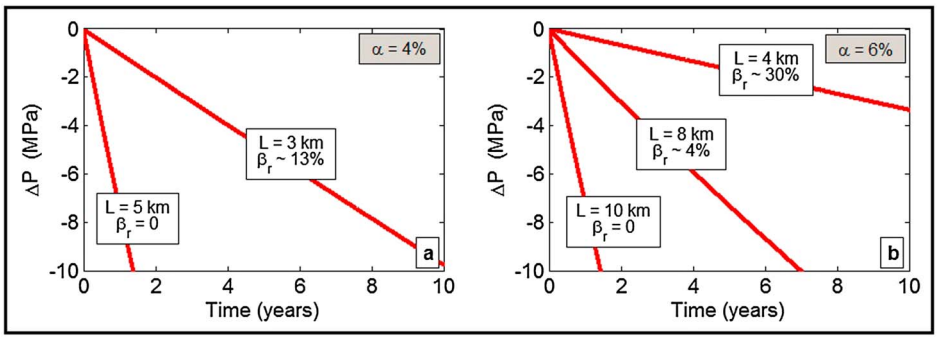

Figure 5. Influence of the exsolution of bubbles in the reservoir on the pressure evolution during quiescence. (a) Underpressure of the reservoir with time for $\alpha = 4$ %, and hence density $\rho_{nd} = 2370$ kg/m^3. For $L = 3$ km, $n_x = n_r = 2.6$ wt %, and $\rho_x = \rho_r = 2530$ kg/m^3; for $L = 5$ km, $n_x = n_r = 0$, and $\rho_x = \rho_{c1} = 2670$ kg/m^3 (gas-magma separation in the upper conduit). (b) Underpressure of the reservoir with time for $\alpha = 6$ %, and hence densities $\rho_{nd} = 2260$ kg/m^3. For $L = 4$ km, $n_x = n_r = 2.1$ wt %, and $\rho_x = \rho_r = 2380$ kg/m^3; for $L = 8$ km, $n_x = n_r = 0.5$ wt %, and $\rho_x = \rho_r = 2290$ kg/m^3; for $L = 10$ km, $n_x = n_r = 0$ and $\rho_x = \rho_{c1} = 2670$ kg/m^3 (gas-magma separation in the upper conduit). β_r is the gas volume fraction in the reservoir, which is $\beta_r = m_{g,r}(t_0)/\hat{\rho}_{g,r}(t_0)V_r(t_0)$. For the rest of the parameters, we have considered the following: $\hat{Q} = 4$ kt/d, $\mu = 10^{18}$ Pa s; $k = 10^{10}$ Pa; $R(t_0) = 40$ m, $V_r(t_0) = 10^9$ m^3; $\gamma_c(t_0) = 1$ (completely degassed magma in the conduit). The initial pressure in the reservoir $P(t_0)$ is calculated as $P(t_0) = gL\rho_{c1}(1 - \beta_c(t_0))$, where $\beta_c(t_0)$ is the initial gas volume fraction in the magma column. The initial volume of melt in the column is $V_{m,c}(t_0) = \pi R(t_0)^2 L(1 - \beta_c(t_0))$. We have used $\beta_c(t_0) = 0.1$.

respectively (for the parameters used in Figure 4). The coupling of our analysis with simple convection models also shows that depressurization induced by degassing can be very significant.

4.2. Scenario 2: Gas Exsolution in the Reservoir, No Replenishment, and Constant Mean Density of Melt in the Column ($n_r(t) \neq 0$, $\lambda(t) = 0$, $\hat{\rho}_{m,c}(t) = \hat{\rho}_{m,c}(t_0)$)

This scenario can correspond to a volcano in which gas-magma separation occurs at depth and bubbles can ascend and escape steadily through a vesicular magma conduit. We found that the shallower the reservoir and the larger the volatile content, the lower the depressurization rate (Figure 5). This is because there is a negative feedback between the depressurization by degassing and the gas content within the reservoir. That is, a gradual and slow depressurization increases the gas content in the reservoir, which in turn pushes more melt into the conduit and tends to reduce the depressurization rate. Reservoirs between 3 and 4 km depth depressurize around 1–2 MPa after 10 years of degassing (for the parameters of Figures 5a and 5b), which contrasts with the fast depressurization of 3 MPa/year for bubble-free reservoirs at depths larger than 4 km if $\alpha = 4$ wt % (Figure 5a), and larger than 10 km if $\alpha = 6$ wt % (Figure 5b). The pressure decrease by degassing is independent of depth for bubble-free reservoirs. We can conclude that depressurization of at least a few MPa can be reached after a few years of passive degassing even if bubbles are present in the reservoir.

4.3. Scenario 3: Gas-Free Reservoir, Magma Replenishment, and Constant Mean Density of Melt in the Column ($n_r(t) = 0$, $\lambda(t) \neq 0$, $\hat{\rho}_{m,c}(t) = \hat{\rho}_{m,c}(t_0)$)

In this section, we investigate how passive degassing may affect magma replenishment if there is a narrow dyke connecting the shallow reservoir with a deeper magma source. First, we analyze a case with constant hydraulic strength and pressure of the source equal to the hydrostatic pressure at time t_0 (see below equation (29)). Second, we explore a simple but more realistic scenario consisting in a variable hydraulic strength with time and an overpressurized deep magma source ($\Delta P_s > 0$).

4.3.1. Constant Hydraulic Strength ($\lambda(t) = \text{constant} > 0$) and $\Delta P_s = 0$

We find that the larger the dyke radius, the lower the depressurization rate (Figure 6a). This occurs because of a negative feedback between depressurization by degassing and the replenishment of magma in the reservoir. That is, a gradual and slow depressurization increases the replenishment rate of magma into the reservoir (see equation (29)), which in turn pushes more melt into the conduit and tends to reduce the depressurization rate. For large enough dyke radius (more than 2–3 m for the parameters of Figure 6), the depressurization tends to zero. In such a case, the volcano would remain during quiescence in a state of ideal pressure balance between the volume change of melt by degassing and the magma volume gained by replenishment. The volume of replenished magma induced by passive degassing, and the rate of magma refilling, can reach values on the order of $V_{rep} \sim 10^6 - 10^7$ m^3 and $dV_{rep}/dt \sim 10 - 20$ m^3/yr, respectively

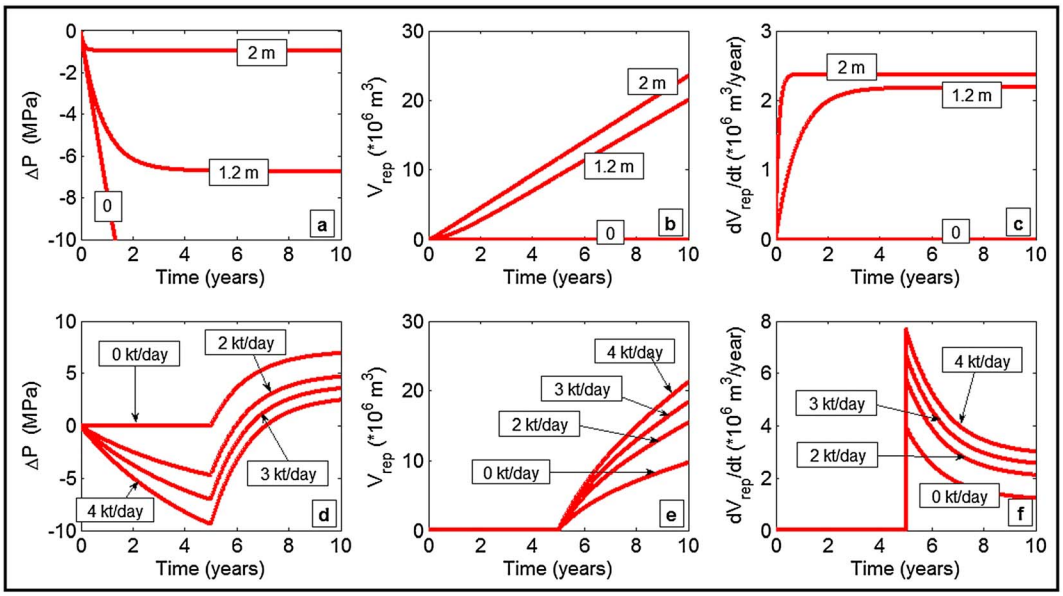

Figure 6. Pressure evolution when the reservoir is hydraulically connected to a deeper magma source. (a) Depressurization for different dyke radius $R_d = 0$, 1.2, and 2 m, for $\Delta P_s(t) = 0$, $\hat{Q} = 4$ kt/d, $R(t_0) = 40$ m, and $V_r(t_0) = 10^9$ m^3. (b) Volume of replenished magma for the same parameters than in Figure 6a. (c) Rate of magma replenishment for the same parameters than in Figure 6a. (d) Pressure evolution for different values of the gas flux, $R_d = 1$ m, $\Delta P_s(t) = 10$ MPa, $R(t_0) = 50$ m, $V_r(t_0) = 5 \times 10^9$ m^3. This is obtained by solving equation (35) numerically. (e) Volume of replenished magma for the same parameters than in Figure 6d. (f) Rate of magma replenishment for the same parameters than in Figure 6d. For the rest of the parameters, we have considered: $\mu_{nd} = 10^{4.2}$ Pa s, $k = 10^{10}$ Pa, $\mu = 10^{18}$ Pa s, $\alpha = 2$ wt %, $n_x = n_c = 2$ wt % (gas-magma separation at the upper conduit), $M = 5000$ m, $\rho_{c1} = 2670$ kg/m^3, $\rho_{c2} = \rho_{nd} = 2500$ kg/m^3, $\gamma_c(t_0) = 0.5$, $T = 1000$°C, and $L = 6$ km. With these parameters, $n_r(t) = 0$.

(Figures 6b and 6c). This finding implies that magma refilling of the reservoir can occur together with depressurization as opposed to pressurization because degassing can decrease the pressure more than what magma replenishment increases it.

4.3.2. Time-Dependent Hydraulic Strength ($\lambda(t)$) and $\Delta P_s > 0$

A more realistic scenario consists in considering changes of the hydraulic strength because the cooling of magma within narrow feeder dykes can be important, thus changing significantly the magma viscosity and the dyke radius. In fact, magma cooling and dyke closure depend not only on the temperature of the host-rock and the initial dyke radius but also on the pressure difference between the source and the reservoir [e.g., *Bruce and Huppert*, 1989], and thus on $\Delta P(t)$. Analyzing the coupling between thermal variations within the dykes, the variations of the hydraulic strength, and ΔP (t), is beyond the scope of this paper, but in Figures 6d and 6f, we assess the effect of depressurization by degassing on the replenishment rates if the reservoir and the deep source become suddenly connected. As we showed so far, the pressure of the shallow reservoir decreases a few MPa during passive degassing at a rate which depends on the gas flux (Figure 6d). And once the reservoir and the deeper source become connected (after 5 years of quiescence in the example of Figure 6), magma moves from the source into the reservoir at a rate which is larger for larger gas fluxes (Figures 6e and 6f). Neglecting depressurization by degassing can lead to underestimations of the volume of replenished magma (and replenishment rate) of up to a factor two (for the parameters used in Figure 6). This simple scenario illustrates the important role that passive degassing can play in the magma intrusion dynamics beneath a volcano.

4.4. Scenario 4: Gas-Free Reservoir, No Replenishment, and Gradually Increasing Mean Density of Melt in the Column ($n_r(t) = 0$, $\lambda(t) = 0$, $\hat{\rho}_{m,c}(t) \neq \hat{\rho}_{m,c}(t_0)$)

The maximum influence of the variation of the density of melt in the conduit $\hat{\rho}_{m,c}(t)$ can be explored by imposing a scenario in which only the magma conduit degasses; namely, gas-magma separation occurs at shallow levels but there is no convection replacing the degassed melt by undegassed melt from the reservoir. In such a case, we obtain that the depressurization is about three times slower than if the density is kept constant (2 MPa versus 6 MPa after 5 years of quiescence for the parameters used in Figure 7a). In any case,

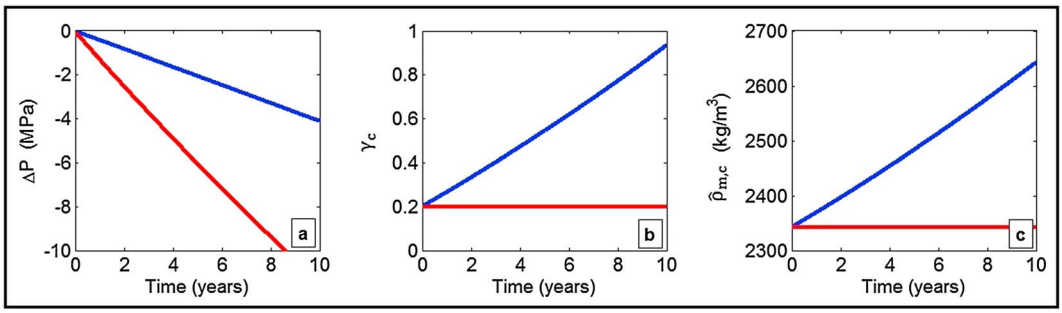

Figure 7. Maximum effect of the density changes of melt in the conduit. Blue lines correspond to the end-member scenario in which the mean density of melt in the conduit increases because the degassed melt at low pressures is not replaced via convection. Red lines correspond to a scenario in which the mean density of melt in the conduit is kept constant. (a) Underpressure of the reservoir with time. (b) Volume fraction of degassed melt in the magma column. (c) Mean density of melt in the magma column. For the parameters, we have considered: $\hat{Q} = 4$ kt/d, $R(t_0) = 70$ m, $V_r(t_0) = 10^9$ m^3, $k = 10^{10}$ Pa, $\mu = 10^{18}$ Pa s, $L = 10$ km, $\alpha = 6$ %, $n_x = n_c = 6$ wt % (gas-magma separation at the upper conduit), $\gamma_c(t_0) = 0.2$, $\rho_x = \rho_{c1} = 2670$ kg/m^3, $\rho_{c2} = \rho_{nd} = 2260$ kg/m^3, $T = 1000$°C.

we can conclude that the pressure in the reservoir can also decrease by several MPa during the intereruptive timescales if the volume fraction of degassed melt ($\gamma_c(t)$) and the mean density of melt in the column ($\hat{\rho}_{m,c}(t)$) increase during passive degassing (Figures 7b and 7c).

5. Discussion

Previous studies investigated the mechanisms that can sustain passive degassing at persistently degassing volcanoes [e.g., *Kazahaya et al*., 1994; *Stevenson and Blake*, 1998; *Edmonds et al*., 2001; *Harris et al*., 2005; *Shinohara and Tanaka*, 2012], or the processes that lead to continuous pressurizations of magma reservoirs [e.g., *Blake*, 1981; *Tait et al*., 1989]. By contrast, we have performed a theoretical analysis that accounts for the mass decrease by degassing, and for different coupled processes that can affect the pressure in the reservoir. On the one hand, degassing decreases the mass of melt within the conduit, which tends to decrease the pressure at depth. On the other hand, a pressure decrease tends to reduce the volume of the system, nucleate and expand bubbles, and induce replenishment if the shallow reservoir and a deep magma source are hydraulically connected. These processes displace more magma and thus more mass into the conduit, such that the resulting pressure change is given by the mass decrease of melt within the conduit due to degassing, and the mass compensation due to the dynamic response of the system. For many scenarios, the mass moving into the conduit does not fully compensate the mass decrease by degassing, and the pressure in the reservoir decreases by several MPa in only a few months or years, i.e., within the intereruptive timescales.

Our lumped-parameter model predicts larger depressurization rates for larger gas fluxes, smaller volcanic systems, lower gas content in the magma reservoir, larger effective viscosities of the crust, and lower hydraulic strengths. In particular, if there are no bubbles in the reservoir and the connectivity between the reservoir and the feeder magma sources is low or null, the depressurization rate is constant for constant gas flux and rigid or elastic rheologies, whereas it decreases with time if the viscous effects of the crust become important. For small volcanic systems ($10^8 - 10^9$ m^3), the depressurization rate can vary between 4 and 10 MPa/year, is not strongly sensitive to the volume of the magmatic system, and varies significantly with the conduit radius. For large volcanic systems ($10^9 - 10^{10}$ m^3), the depressurization is generally lower (up to ~5–10 MPa in several years) and is very sensitive to the reservoir volume and the effective viscosity of the crust. Gas exsolution in the reservoir tends to decrease the depressurization rate, even though underpressures of several MPa can be still reached after a few years. Our model also shows that magma replenishment rates of volcanic reservoirs can be enhanced by degassing-induced depressurization and that neglecting degassing leads to a significant underestimation of the volume of replenished magma. Even if the mean density of melt increases progressively with time, the depressurization can be on the order of several MPa during quiescence.

Various observations and geophysical data at several volcanoes are consistent with important mass decreases within the conduit and pressure drops during quiescent degassing. For instance, at Satsuma-Iwojima volcano

(Japan), a crack opened at the summit of the volcanic edifice on June 1996, which was interpreted as a pressure decrease beneath the crater [*Iguchi et al*., 2002]; a very low density region, thought to be the result of collapsed material, was found up to 100 m below the crater floor by means of muon tomography [*Tanaka et al*., 2010], and a low gravity anomaly has been recorded at the active cone [*Shinohara and Tanaka*, 2012]. At Mount Asama (Japan), there were successive collapses of the crater floor after the eruption of 2004 ended and up to January 2006 [*Urabe et al*., 2006; *Tanaka et al*., 2010], and a very low density region of up to 200 m was also found below the crater floor [*Tanaka et al*., 2008]. The very low density regions found beneath Satsuma-Iwojima and Asama craters could be consequence of a magma level drop in the conduit during quiescence. This is a possibility that is also predicted by our model. Indeed, if we neglect the short-term rise and fall of the magma level due to the complex bubble dynamics within the conduit [e.g., *Dibble*, 1972; *Jaupart and Vergniolle*, 1988; *Orr and Rea*, 2012], there is a correlation between the pressure change in the reservoir and the change of magma level. If for simplicity we neglect changes of the radius and changes of the melt density, and we use that the mass of melt in the conduit is much larger than the mass of gas, we can get easily from equation (1) that the magma level drop is given by $|\Delta P(t)|/g\hat{\rho}_{m,c}$. Hence, magma level drops of 100 m, like in Satsuma-Iwojima, and 200 m, like in Asama, correspond to pressure drops of around 2.5 and 5 MPa, respectively. These values are consistent with the depressurization induced by degassing that we have obtained.

Another example of depressurization during passive degassing is found in Llaima volcano (Chile), where subsidence of the volcanic edifice on the order of 10^7 m^3 was recorded during three years and a half (from November 2003 to May 2007) before a fast inflation lasting for six months and the onset of an eruption [*Bathke et al*., 2011]. The subsidence is consistent with the volume decrease predicted for the reservoir by our model assuming elastic or viscoelastic rheology for the crust (see Figure 2b). Factors such as the regional stress field and very shallow processes near pit craters may cause more complex deformations and may complicate the interpretation of data [*Battaglia and Segall*, 2004], and thus, lack of deflation does not mean necessarily that there is no depressurization by degassing. That is the case of Masaya volcano (Nicaragua), where periods of passive degassing without deflation have been monitored, but recurrent collapses of the crater floor occur as consequence of cavernous structures located below [*Rymer et al*., 1998]. Microgravimetric data from Masaya also noted anomalies from 1993 to 1994 consistent with shallow mass decreases by gas loss [*Rymer et al*., 1998], and another gravity decrease was recorded from 1997 to 1999 and previously attributed to changes in vesicularity of the upper conduit [*William-Jones et al*., 2003].

A question that arises naturally from our theoretical analysis is whether depressurization by passive degassing can trigger the onset of different processes that lead to new unrest episodes and eruptions. We propose below three processes we think could be triggered by degassing-induced depressurization after a few months or years of quiescence and that require further study in the future.

First, degassing-induced depressurization could be responsible for the sudden replenishment discussed in Figures 6d–6f if we consider that the magma initially filling the connecting dykes has a Bingham rheology because it is cold and crystal rich [*Melnik and Sparks*, 2005]. In such a case, magma within the dykes acts as a solid plug as long as the pressure difference between the source and the shallow reservoir ($\Delta P_s\,(t) - \Delta P\,(t)$) does not exceed a threshold value, which could occur if the pressure in the reservoir decreases sufficiently after a few months or years of quiescence. The threshold pressure difference to unplug the dykes and initiate magma ascent can range between much less than 1 MPa and more than 30 MPa depending on the yield strength, the geometry of the dykes, cooling, and the crystal distribution [*Melnik and Sparks*, 2005].

Second, gradual depressurization by quiescent steady state degassing leads to gradual deepening of the exsolution level within the volcanic system, which can favor the transport of volatiles between different magma layers, and in turn affect the degassing rates [*Simakin and Botcharnikov*, 2001]. The deepening of the exsolution level also implies that the volume of magma able to exsolve volatiles depends on how the section of the conduit and reservoir vary with depth. For example, if the exsolution level moves from the bottom of the conduit to the top of the reservoir, we can expect a sudden increase of the volume of bubbly magma because of the larger cross-section of the reservoir. In turn, this may lead to ascent of magma towards the surface and pressurizations at shallow depths, which could induce explosions [e.g., *Namiki and Manga*, 2005].

Third, depressurization can induce cracking and sudden subsidence of the reservoir roof if the difference between the pressure of the reservoir ($P(t_0) + \Delta P(t)$) and the lithostatic pressure at reservoir depths (P_{Lit}) reaches the strength of rocks (σ) [*Blake*, 1981]. If we consider that initially the reservoir is in equilibrium with

the surrounding crust ($P(t_0) = P_{Lit}$), the criteria for wall-rock failure would be simply $|\Delta P(t)| = \sigma$. The strength of rocks σ varies between 0.5 and 9 MPa when the rocks are subjected to tensile stresses [*Gudmundsson*, 2012], which are the stresses that develop around loaded cavities [*Carter et al*., 1991] or around reservoirs subjected to the load of a volcanic edifice [*Pinel and Jaupart*, 2005]. These values of the rock strength are consistent with the order of magnitude of the pressure changes caused by degassing. Degassing-induced depressurization can also induce crater collapse [*Iguchi et al*., 2002] and seismicity by poroelastic stressing, as it was proposed for the earthquakes that occurred near the Lacq gas field in France after gas extraction [*Segall et al*., 1994].

6. Conclusions

We have presented a new lumped-parameter model that captures the long-term (from months to years) pressure changes induced by passive degassing in volcanic magma reservoirs. Our model demonstrates that degassing-induced depressurization can reach values on the order of several MPa in the intereruptive timescales (<10 years), which is consistent with the geophysical and geodetical observations (e.g., edifice deflation, very low density at the upper part of the conduit, or crater floor collapse) of several persistently degassing volcanoes. Our results suggest that the unrest episodes and eruptions occurring every few months or years at persistently degassing volcanoes could be triggered by a variety of physical processes that are promoted by degassing-induced depressurization during quiescence. Passive degassing could induce magma replenishment, sudden gas exsolution at depth, and cracking and sudden subsidence of the crater floor or reservoir wall-rock. The challenge for the future is to explore these processes through numerical and analog models.

Notation

Symbol	Description	Range
ΔP	pressure change during quiescence	≤ 10 MPa (absolute value)
$\hat{Q}$	total mean gas flux	1–10 kt/d
t	time of passive degassing	≤ 10 years
R	volcanic conduit radius	10–100 m
V_r	volume of the reservoir	10^7–10^{10} m^3
L	length of the magma column (up to the average reservoir depth)	3–10 km
α	mass fraction of dissolved volatiles in parent melt	1– 6 wt %
k	bulk modulus of rocks	10^{10}–10^{11} Pa
μ	effective viscosity of the crust	$10^{17} - 10^{21}$ Pa s
g	gravity	9.8 m/s^2
$\hat{\rho}_{m,c}$	mean density of melt inside the magma column	2200–2800 kg/m^3
$\hat{\rho}_{g,c}$	mean density of gas inside the magma column	≤ 200 kg/m^3
ρ_{c1}	density of the fully degassed melt in the column	2500–2800 kg/m^3
ρ_{c2}	density of partially degassed melt in the column	2200–2600 kg/m^3
$\Delta\rho_{1,2}$	difference between ρ_{c1} and ρ_{c2}	50–400 kg/m^3
ρ_{nd}	density of the parent undegassed melt	2200–2800 kg/m^3
ρ_r	density of the melt that degasses in the reservoir	$\rho_r \leq \rho_{c1}$
ρ_x	density of melt at the gas-magma separation level	$\rho_x = \rho_{c1}$ or $\rho_x = \rho_r$
$\hat{\rho}_{g,r}$	mean density of gas in the reservoir	≤ 200 kg/m^3
n_c	wt % of water exsolved in the upper conduit	$\leq \alpha$
n_r	wt % of water exsolved in the reservoir	$n_r < n_c \leq \alpha$
n_x	wt % of water exsolved in the reservoir or conduit	$n_x = n_c$ or $n_x = n_r$
γ_c	volume fraction of degassed melt in the magma column	0–1
μ_{nd}	viscosity of the undegassed parent melt	10^2–10^5 Pa s
μ_1	viscosity of the degassed melt in the conduit	$> \mu_{nd}$
R_d	radius of the dyke	≤ 5 m
M	length of the dykes	2–6 km
R^*	empirical constant [*Stevenson and Blake*, 1998]	0.6
ξ	poiseuille number [*Stevenson and Blake*, 1998]	0.064
M_{H_2O}	molecular weight of water	18 g/mol
T	temperature of the magma	900–1200 ℃
S	constant of the Henry's law for water	4×10^{-6} Pa$^{-1/2}$
R_g	universal gas constant	8.31 J/(K mol)
A^*	indicator variable	0 or 1
B^*	indicator variable	0 or 1

ΔP_∞	maximum pressure change
Γ	parameter defined in equation (39)
ρ_w	parameter defined in equation (20)
$m_{g,c}$	mass of gas within the column of length L
$m_{m,c}$	mass of melt within the column of length L
$m_{g,r}$	mass of gas in the reservoir
$V_{g,c}$	volume of gas inside the column of length L
$V_{g,r}$	volume of gas that exsolves in the reservoir
$V_{m,c}$	volume of melt inside the column of length L
$V_{m,c1}$	volume of fully degassed melt inside the column of length L
$dV_{undeg}/dt\|_d$	volume change of undegassed melt in the system due to degassing
dV_{deg}/dt	volume change of fully degassed melt in the system
dV_d/dt	volume decrease of melt in the system due to gas exsolution
V_m	volume of melt in the conduit-reservoir
$V_{m,r}$	volume of melt in the reservoir
V_{rep}	volume of replenished melt
D	portion of the magma column which is within the reservoir
β_r	gas volume fraction in the reservoir
β_c	gas volume fraction in the magma column
P_{Lit}	lithostatic pressure at reservoir depths
σ	strength of rocks
λ	hydraulic strength

Acknowledgments

The Matlab scripts to plot Figures 2–7 are available in the supporting material. We thank C. Huber and G. Schubert for discussion and comments on the subjects of this manuscript. We appreciate the comments and suggestions of S. Blake, J. Vandemeulebrouck, M. Manga, and one anonymous reviewer that helped to improve the manuscript. Support from the Agency for Science, Technology, and Research (A*STAR, Singapore), and the Earth Observatory of Singapore (Magma Plumbing System Project), is gratefully acknowledged.

References

Aiuppa, A., R. Moretti, C. Federico, G. Giudice, S. Gurrieri, M. Liuzzo, P. Papale, H. Shinohara, and M. Valenza (2007), Forecasting Etna eruptions by real-time observation of volcanic gas composition, *Geology*, *35*, 1115–1118, doi:10.1130/G24149A.1.

Aiuppa, A., G. Giudice, S. Gurrieri, M. Liuzzo, M. Burton, T. Caltabiano, A. J. S. McGonigle, G. Salerno, H. Shinohara, and M. Valenza (2008), Total volatile flux from Mount Etna, *Geophys. Res. Lett.*, *35*, L24302, doi:10.1029/2008GL035871.

Allard, P., J. Carbonnelle, N. Métrich, H. Loyer, and P. Zettwoog (1994), Sulphur output and magma degassing budget of Stromboli volcano, *Nature*, *368*, 326–330, doi:10.1038/368326a0.

Andres, R. J., and A. D. Kasgnoc (1998), A time-averaged inventory of subaerial volcanic sulfur emissions, *J. Geophys. Res.*, *103*, 25,251–25,261, doi:10.1029/98JD02091.

Bathke, H., M. Shirzaei, and T. R. Walter (2011), Inflation and deflation at the steep-sided Llaima stratovolcano (Chile) detected by using InSAR, *Geophys. Res. Lett.*, *38*, L10304, doi:10.1029/2011GL047168.

Battaglia, M., and P. Segall (2004), The interpretation of gravity changes and crustal deformation in active volcanic areas, *Pure Appl. Geophys.*, *161*, 1453–1467, doi:10.1007/s00024-004-2514-5.

Blake, S. (1981), Volcanism and the dynamics of open magma chambers, *Nature*, *289*, 783–785, doi:10.1038/289783a0.

Boichu, M., C. Oppenheimer, V. Tsanev, and P. R. Kyle (2010), High temporal resolution SO_2 flux measurements at Erebus volcano, Antarctica, *J. Volcanol. Geotherm. Res.*, *190*, 325–336, doi:10.1016/j.jvolgeores.2009.11.020.

Bruce, P. M., and H. E. Huppert (1989), Thermal control of basaltic fissure eruptions, *Nature*, *342*, 665–667, doi:10.1038/342665a0.

Burton, M. R., C. Oppenheimer, L. A. Horrocks, and P. W. Francis (2000), Remote sensing of CO_2 and H_2O emission rates from Masaya volcano, Nicaragua, *Geology*, *28*, 915–918, doi:10.1130/0091-7613(2000)28<915:RSOCAH>2.0.CO;2.

Burton, M. R., H. M. Mader, and M. Polacci (2007), The role of gas percolation in quiescent degassing of persistently active basaltic volcanoes, *Earth Planet. Sci. Lett.*, *264*, 46–60, doi:10.1016/j.epsl.2007.08.028.

Carter, B. J., E. Z. Lajtai, and A. Petukhov (1991), Primary and remote fracture around underground cavities, *Int. J. Numer. Anal. Meth. Geomech.*, *15*, 21–40, doi:10.1002/nag.1610150103.

Costa, A., and G. Macedonio (2003), Viscous heating in fluids with temperature-dependent viscosity: Implications for magma flows, *Nonlinear Proc. Geophys.*, *10*, 545–555.

Del Negro, C., G. Currenti, and D. Scandura (2009), Temperature-dependent viscoelastic modeling of ground deformation: Application to Etna volcano during the 1993–1997 inflation period, *Phys. Earth Planet. Inter.*, *172*, 299–309, doi:10.1016/j.pepi.2008.10.019.

Dibble, R. R. (1972), Seismic and related phenomena at active volcanoes in New Zealand, Hawaii, and Italy, PhD dissertation, Victoria Univ., Wellington.

Divoux, T., V. Vidal, M. Ripepe, and J. C. Géminard (2011), Influence of non-Newtonian rheology on magma degassing, *Geophys. Res. Lett.*, *38*, L12301, doi:10.1029/2011GL047789.

Dzurisin, D. (2007), *Volcano Deformation—Geodetic Monitoring Techniques*, Springer, Berlin.

Edmonds, M., D. Pyle, and C. Oppenheimer (2001), A model for degassing at the Soufriere Hills Volcano, Montserrat, West Indies, based on geochemical data, *Earth Planet. Sci. Lett.*, *186*, 159–173, doi:10.1016/S0012-821X(01)00242-4.

Galle, B., C. Oppenheimer, A. Geyer, A. S. J. McGonigle, M. Edmonds, and L. A. Horrocks (2002), A miniaturised ultraviolet spectrometer for remote sensing of SO_2 fluxes: A new tool for volcano surveillance, *J. Volcanol. Geotherm. Res.*, *119*, 241–254, doi:10.1016/S0377-0273(02)00356-6.

Galle, B., M. Johansson, C. Rivera, Y. Zhang, M. Kihlman, C. Kern, T. Lehmann, U. Platt, S. Arellano, and S. Hidalgo (2010), Network for Observation of Volcanic and Atmospheric Change (NOVAC)—A global network for volcanic gas monitoring: Network layout and instrument description, *J. Geophys. Res.*, *115*, D05304, doi:10.1029/2009JD011823.

Ghiorso, M. S., and R. O. Sack (1995), Chemical mass transfer in magmatic processes. IV. A revised and internally consistent thermodynamic model for the interpolation and extrapolation of liquid–solid equilibria in magmatic systems at elevated temperatures and pressures, *Contrib. Mineral. Petrol.*, *119*, 197–212, doi:10.1007/BF00307281.

Gudmundsson, A. (2012), Magma chambers: Formation, local stresses, excess pressures, and compartments, *J. Volcanol. Geotherm. Res.*, *237–238*, 19–41, doi:10.1016/j.jvolgeores.2012.05.015.

Harris, A., and M. Ripepe (2007), Temperature and dynamics of degassing at Stromboli, *J. Geophys. Res.*, *112*, B03205, doi:10.1029/2006JB004393.
Harris, A. J. L., R. Carniel, and J. Jones (2005), Identification of variable convective regimes at Erta Ale Lava Lake, *J. Volcanol. Geotherm. Res.*, *142*, 207–223, doi:10.1016/j.jvolgeores.2004.11.011.
Huppert, H. E., and A. W. Woods (2002), The role of volatiles in magma chamber dynamics, *Nature*, *420*, 493–495, doi:10.1038/nature01211.
Iguchi, M., E. Saito, Y. Nishi, and T. Tameguri (2002), Evaluation of recent activity at Satsuma-Iwojima—Felt earthquake on June 8, 1996, *Earth Planets Space*, *54*, 187–195.
James, M. R., S. J. Lane, and B. A. Chouet (2006), Gas slug ascent through changes in conduit diameter: Laboratory insights into a volcano-seismic source process in low-viscosity magmas, *J. Geophys. Res.*, *111*, B05201, doi:10.1029/2005JB003718.
Jaupart, C., and S. Vergniolle (1988), Laboratory models of Hawaiian and Strombolian eruptions, *Nature*, *331*, 58–60, doi:10.1038/331058a0.
Jellinek, A. M., and D. J. DePaolo (2003), A model for the origin of large silicic magma chambers: precursors of caldera-forming eruptions, *Bull. Volcanol.*, *65*, 363–381, doi:10.1007/s00445-003-0277-y.
Johansson, M., B. Galle, Y. Zhang, C. Rivera, D. Chen, and K. Wyser (2009), The dual-beam mini-DOAS technique-measurements of volcanic gas emission, plume height and plume speed with a single instrument, *Bull. Volcanol.*, *71*, 747–751, doi:10.1007/s00445-008-0260-8.
Kavanagh, J. L., and R. S. J. Sparks (2011), Insights of dyke emplacement mechanics from detailed 3D dyke thickness datasets, *J. Geol. Soc.*, *168*, 965–978, doi:10.1144/0016-76492010-137.
Kazahaya, K., H. Shinohara, and G. Saito (1994), Excessive degassing of Izu-Oshima volcano: Magma convection in a conduit, *Bull. Volcanol.*, *56*, 207–216, doi:10.1007/BF00279605.
Kazahaya, K., H. Shinohara, and G. Saito (2002), Degassing process of Satsuma-Iwojima volcano, Japan: Supply of volatile components from a deep-magma chamber, *Earth Planets Space*, *54*, 327–355.
Lipman, P. W., N. G. Banks, and J. M. Rhodes (1985), Degassing-induced crystallization of basaltic magma and effects on lava rheology, *Nature*, *317*, 604–607, doi:10.1038/317604a0.
Martin, R. S., et al. (2010), A total volatile inventory for Masaya volcano, Nicaragua, *J. Geophys. Res.*, *115*, B09215, doi: 10.1029/2010JB007480.
Melnik, O., and R. S. J. Sparks (2005), Controls on conduit magma flow dynamics during lava dome building eruptions, *J. Geophys. Res.*, *110*, B02209, doi:10.1029/2004JB003183.
Metrich, N., A. Bertagnini, P. Landi, and M. Rosi (2001), Crystallization driven by decompression and water loss at Stromboli volcano (Aeolian Islands, Italy), *J. Petrol.*, *42*, 1471–1490, doi:10.1093/petrology/42.8.1471.
Namiki, A., and M. Manga (2005), Response of a bubble bearing viscoelastic fluid to rapid decompression: Implications for explosive volcanic eruptions, *Earth Planet. Sci. Lett.*, *236*, 269–284, doi:10.1016/j.epsl.2005.02.045.
Newman, A. V., T. H. Dixon, G. I. Ofoegbu, and J. E. Dixon (2001), Geodetic and seismic constraints on recent activity at Long Valley Caldera, California: Evidence for viscoelastic rheology, *J. Volcanol. Geotherm. Res.*, *105*, 183–206, doi:10.1016/S0377-0273(00)00255-9.
Okumura, S., M. Nakamura, A. Tsuchiyama, T. Nakano, and K. Uesugi (2008), Evolution of bubble microstructure in sheared rhyolite: Formation of a channel-like bubble network, *J. Geophys. Res.*, *113*, B07208, doi:10.1029/2007JB005362.
Oppenheimer, C., P. Francis, M. Burton, A. J. H. Maciejewski, and L. Boardman (1998), Remote measurement of volcanic gases by Fourier transform infrared spectroscopy, *Appl. Phys. B*, *67*, 505–515, doi:10.1007/s003400050536.
Orr, T., and J. C. Rea (2012), Time-lapse camera observations of gas piston activity at Pu'u'Ō'ō, Kīlauea volcano, Hawai'i, *Bull. Volcanol.*, *74*, 2353–2362, doi:10.1007/s00445-012-0667-0.
Pallister, J. S., R. P. Hoblitt, D. R. Crandell, and D. R. Mullineaux (1992), Mount St. Helens a decade after the 1980 eruptions: Magmatic models, chemical cycles, and a revised hazard assessment, *Bull. Volcanol.*, *54*, 126–146, doi:10.1007/BF00278003.
Patrick, M., D. Wilson, D. Fee, T. Orr, and D. Swanson (2011), Shallow degassing events as a trigger for very-long-period seismicity at Kīlauea Volcano, Hawai'i, *Bull. Volcanol.*, *73*, 1179–1186, doi:10.1007/s00445-011-0475-y.
Pinel, V., and C. Jaupart (2005), Caldera formation by magma withdrawal from a reservoir beneath a volcanic edifice, *Earth Planet. Sci. Lett.*, *230*, 273–287, doi:10.1016/j.epsl.2004.11.016.
Pinel, V., C. Jaupart, and F. Albino (2010), On the relationship between cycles of eruptive and growth of a volcanic edifice, *J. Volcanol. Geotherm. Res.*, *194*, 150–164, doi:10.1016/j.jvolgeores.2010.05.006.
Pioli, L., C. Bonadonna, B. J. Azzopardi, J. C. Phillips, and M. Ripepe (2012), Experimental constraints on the outgassing dynamics of basaltic magmas, *J. Geophys. Res.*, *117*, B03204, doi:10.1029/2011JB008392.
Polacci, M., D. R. Baker, A. La Rue, L. Mancini, and P. Allard (2012), Degassing behaviour of vesiculated basaltic magmas: An example from Ambrym volcano, Vanuatu Arc, *J. Volcanol. Geotherm. Res.*, *233–234*, 55–64, doi:10.1016/j.jvolgeores.2012.04.019.
Rymer, H., B. Van Wyk de Vries, J. Stix, and G. Williams-Jones (1998), Pit crater structure and processes governing persistent activity at Masaya Volcano, Nicaragua, *Bull. Volcanol.*, *59*, 345–355, doi:10.1007/s004450050196.
Sawyer, G. M., S. A. Carn, V. I. Tsanev, C. Oppenheimer, and M. Burton (2008), Investigation into magma degassing at Nyiragongo volcano, Democratic Republic of the Congo, *Geochem. Geophys. Geosyst.*, *9*, Q02017, doi:10.1029/2007GC001829.
Segall, P., J. R. Grasso, and A. Mossop (1994), Poroelastic stressing and induced seismicity near the Lacq gas field, southwestern France, *J. Geophys. Res.*, *99*, 15,423–15,438, doi:10.1029/94JB00989.
Shinohara, H. (2008), Excess degassing from volcanoes and its role on eruptive and intrusive activity, *Rev. Geophys.*, *46*, RG4005, doi:10.1029/2007RG000244.
Shinohara, H., and H. Tanaka (2012), Conduit magma convection of a rhyolitic magma: Constraints from cosmic-ray muon radiography of Iwodake, Satsuma-Iwojima volcano, Japan, *Earth Planet. Sci. Lett.*, *349–350*, 87–97, doi:10.1016/j.epsl.2012.07.002.
Siebert, L., T. Simkin, and P. Kimberly (2010), *Volcanoes of the World*, 3rd ed., Univ. Calif. Press, Berkeley.
Simakin, A., and R. Botcharnikov (2001), Degassing of stratified magma by compositional convection, *J. Volcanol. Geotherm. Res.*, *105*, 207–224, doi:10.1016/S0377-0273(00)00256-0.
Sparks, R. S. J. (1978), Dynamics of bubble formation and growth in magmas—Review and analysis, *J. Volcanol. Geotherm. Res.*, *3*, 1–37, doi:10.1016/0377-0273(78)90002-1.
Sparks, R. S. J. (2003), Forecasting volcanic eruptions, *Earth Planet. Sci. Lett.*, *210*, 1–15, doi:10.1016/S0012-821X(03)00124-9.
Stevenson, D. S., and S. Blake (1998), Modelling the dynamics and thermodynamics of volcanic degassing, *Bull. Volcanol.*, *60*, 307–317, doi:10.1007/s004450050234.
Stoiber, R. E., L. L. Malinconico, and S. N. Williams (1983), Use of the correlation spectrometer at volcanoes, in *Forecasting Volcanic Events*, edited by H. Tazieff and J. C. Sabroux, pp. 425–444, Elsevier, New York.
Symonds, R. B., W. I. Rose, G. J. S. Bluth, and T. M. Gerlach (1994), Volcanic-gas studies: methods, results, and applications, in *Volatiles in Magmas, Reviews in Mineralogy and Geochemistry*, vol. 30, edited by M. R. Carroll and J. R. Holloway, pp. 1–66, Mineralog. Soc. of Am., Washington.

Tait, S., C. Jaupart, and S. Vergniolle (1989), Pressure, gas content and eruption periodicity of a shallow, crystallising magma chamber, *Earth Planet. Sci. Lett.*, *92*, 107–123, doi:10.1016/0012-821X(89)90025-3.

Tanaka, H. K. M., et al. (2008), Radiographic imaging below a volcanic crater floor with cosmic-ray muons, *Am. J. Sci.*, *308*, 843–850, doi:10.2475/07.2008.02.

Tanaka, H. K. M., T. Uchida, M. Tanaka, H. Shinohara, and H. Taira (2009), Cosmic-ray muon imaging of magma in a conduit: Degassing process of Satsuma-Iwojima Volcano, Japan, *Geophys. Res. Lett.*, *36*, L01304, doi:10.1029/2008GL036451.

Tanaka, H. K. M., T. Uchida, M. Tanaka, H. Shinohara, and H. Taira (2010), Development of a portable assembly-type cosmic-ray muon module for measuring the density structure of a column of magma, *Earth Planets Space*, *62*, 119–129, doi:10.5047/eps.2009.06.003.

Touloukian, Y. S., W. R. Judd, and R. F. Roy (1981), *Physical Properties of Rocks and Minerals*, McGraw Hill, New York.

Urabe, B., W. Watanabe, and M. Murakami (2006), Topographic change of the summit crater of Asama volcano during the 2004 eruption derived from airborne synthetic aperture radar (SAR) measurements, *Bull. Geogr. Surv. Inst. Japan*, *53*, 1–6.

Vergniolle, S., and C. Jaupart (1986), Separated two-phase flow and basaltic eruptions, *J. Geophys. Res.*, *91*, 12,842–12,860, doi:10.1029/JB091iB12p12842.

Walker, J. A., S. N. Williams, R. I. Kalamarides, and M. D. Feigenson (1993), Shallow open-system evolution of basaltic magma beneath a subduction zone volcano—The Masaya caldera complex, Nicaragua, *J. Volcanol. Geotherm. Res.*, *56*, 379–400, doi:10.1016/0377-0273(93)90004-B.

William-Jones, G., H. Rymer, and D. Rothery (2003), Gravity changes and passive SO_2 degassing at the Masaya caldera complex, Nicaragua, *J. Volcanol. Geotherm. Res.*, *123*, 137–160, doi:10.1016/S0377-0273(03)00033-7.

Witter, J. B., V. C. Kress, and C. G. Newhall (2005), Volcan Popocatepetl, Mexico. Petrology, magma mixing, and immediate source of volatiles for the 1994-Present eruption, *J. Petrol.*, *46*, 2337–2366, doi:10.1093/petrology/egi058.

Young, W. C., and R. G. Budynas (2002), *Roark's Formulas for Stress and Strain*, 7th ed., McGraw Hill, New York.